Unravelling the mechanisms controlling Cd accumulation and Cd-tolerance in Brachiaria decumbens and Panicum maximum under summer and winter conditions

Journal:	*Physiologia Plantarum*
Manuscript ID	PPL-2020-00171-HM03.R1
Manuscript Type:	Special Issue article
Date Submitted by the Author:	n/a
Complete List of Authors:	Rabêlo, Flávio Henrique Silveira; University of Sao Paulo Luiz de Queiroz College of Agriculture, Soil Science Gaziola, Salete; University of Sao Paulo Luiz de Queiroz College of Agriculture Rossi, Monica; University of Sao Paulo Centre for Nuclear Energy in Agriculture Silveira, Neidiquele; Institute of Agronomy Wójcik, Małgorzata; Maria Curie-Sklodowska University in Lublin Faculty of Biology and Biotechnology Bajguz, Andrzej; University of Bialystok, Department of Plant Biochemistry; Piotrowska-Niczyporuk, A Lavres, Jose; Center for Nuclear Energy in Agriculture CENA, University of Sao Paulo USP, Piracicaba, Brazil Linhares, Francisco; University of Sao Paulo Centre for Nuclear Energy in Agriculture Azvedo, RA Vangronsveld, Jaco Alleoni, Luís Reynaldo; University of Sao Paulo Luiz de Queiroz College of Agriculture
Key Words:	Antioxidants, Glutathione, Phytochelatins, Photosynthesis, Root apoplast

Unravelling the mechanisms controlling Cd accumulation and Cd-tolerance in *Brachiaria decumbens* and *Panicum maximum* under summer and winter weather conditions

Flávio Henrique Silveira Rabêlo[a,b,*], Salete Aparecida Gaziola[a], Monica Lanzoni Rossi[c], Neidiquele Maria Silveira[d], Małgorzata Wójcik[e], Andrzej Bajguz[f], Alicja Piotrowska-Niczyporuk[f], José Lavres[c], Francisco Scaglia Linhares[c], Ricardo Antunes Azevedo[a], Jaco Vangronsveld[b], Luís Reynaldo Ferracciú Alleoni[a]

[a] University of São Paulo, College of Agriculture Luiz de Queiroz, Piracicaba, Brazil
[b] Hasselt University, Centre for Environmental Sciences, Diepenbeek, Belgium
[c] University of São Paulo, Center for Nuclear Energy in Agriculture, Piracicaba, Brazil
[d] Agronomic Institute, Center R&D in Ecophysiology and Biophysics, Campinas, Brazil
[e] Maria Curie-Skłodowska University, Faculty of Biology and Biotechnology, Lublin, Poland
[f] University of Bialystok, Faculty of Biology and Chemistry, Białystok, Poland

Correspondence
*Corresponding author,
E-mail: flaviohsr.agro@usp.br

We evaluated the mechanisms that control Cd accumulation and distribution, and the mechanisms that protect the photosynthetic apparatus of *Brachiaria decumbens* Stapf. cv. Basilisk and *Panicum maximum* Jacq. cv. Massai from Cd-induced oxidative stress, as well as the effects of simulated summer or winter conditions on these mechanisms. Both grasses were grown in unpolluted and Cd-polluted Oxisol (0.63 and 3.6 mg Cd kg^{-1} soil, respectively) at summer and winter conditions. Grasses grown in the Cd-polluted Oxisol presented higher Cd concentration in their tissues in the winter conditions, but the shoot biomass production of both grasses was not affected by the experimental conditions. Cadmium was more accumulated in the root apoplast than the root symplast, contributing to increase the diameter and cell layers of the cambial region of both grasses. Roots of *B. decumbens* were more susceptible to disturbed nutrients uptake and nitrogen metabolism than roots of *P. maximum*. Both grasses translocated high amounts of Cd to their shoots resulting in oxidative stress. Oxidative stress in the leaves of both grasses was higher in summer than winter, but only in *P. maximum* superoxide dismutase (SOD) and ascorbate peroxidase (APX) activities were increased. However, CO_2 assimilation was not affected due to the protection provided by reduced glutathione (GSH) and phytochelatins (PCs) that were more synthesized in shoots than roots. In summary, the root apoplast was not sufficiently effective to prevent Cd translocation from roots to shoot, but GSH and PCs provided good protection for the photosynthetic apparatus of both grasses.

Abbreviations – *A*, leaf CO_2 assimilation; APX, ascorbate peroxidase; AsA, ascorbic acid; BRs, brassinosteroids; BSA, bovine serum albumin; CAT, catalase; Chl, chlorophyll; C_i, intracellular CO_2 concentration; *E*, transpiration; GPX, guaiacol peroxidase; GR, glutathione reductase; g_s, stomatal conductance; GSH, reduced glutathione; GS, glutathione synthetase; GSSG, oxidized glutathione; ICP-OES, inductively coupled plasma optical emission spectrometry; *k*, instantaneous carboxylation efficiency; MDA, malondialdehyde; NUE, nutrient use efficiency; PCs, phytochelatins; PCS, phytochelatin synthase; PEPcase, phosphoenolpyruvate carboxylase; PSI, photosystem I; PSII, photosystem II; SOD, superoxide dismutase; WUE, instantaneous water use efficiency; WUE_i, intrinsic water use efficiency.

Introduction

The use of non-hyperaccumulator plants possessing high biomass production for cadmium (Cd) phytoextraction increased in recent years (Rabêlo et al. 2018a, Suman et al. 2018, Bora et al. 2020). Among the C_4 forage grasses that were investigated, *Brachiaria decumbens* Stapf. cv. Basilisk and *Panicum maximum* Jacq. cv. Massai tolerated very high Cd concentrations in hydroponics (Kopittke et al. 2010, Santos et al. 2011, Rabêlo et al. 2017a, 2017b, 2017c, 2018b, 2018c, 2018d, 2019, 2020). However, the mechanisms that allow them to cope with Cd-induced stress are still poorly understood, especially under environmentally realistic conditions.

Cadmium uptake by plants from the soil includes diffusion of Cd into the free space of the root cells and Cd adsorption by the cell walls (apoplastic uptake), followed by Cd transport across the plasma membrane into the protoplast (symplastic uptake; Lux et al. 2011, Song et al. 2017). Both apoplastic uptake and short-distance transport in the roots and long-distance Cd translocation through the xylem from roots to shoots are mainly transpiration-driven processes. By consequence, conditions that increase leaf transpiration, such as higher temperature, may lead to a higher Cd entrance into the roots and translocation to the shoots in Poaceae (Ge et al. 2016, Guo et al. 2019). The possible higher Cd uptake by plants growing at high temperature could intensify nutritional disturbances, among other damages, since Cd competes with nutrients (e.g. Ca, Fe and Zn) for the same transporters (Carvalho et al. 2020). To avoid nutritional disturbances Cd-induced, plants of the family Poaceae limit Cd translocation from roots to shoots, by e.g. increasing suberinization of the endoderm cells and lignification of the cortex cells and peripheral tissues of root vascular cylinder (Lux et al. 2011, Kaznina and Titov 2014). Gomes et al. (2011) reported that *B. decumbens* grown in soil polluted with Cd, Pb, Zn and Cu showed more lignin deposited in the walls of the root cortical cells compared to control plants. However, there exist no reports on the mechanisms that prevent radial transport and translocation of Cd from roots to shoots in *B. decumbens* exposed to Cd only. Rabêlo et al. (2018b) reported that vascular parenchyma cells of roots of *P. maximum* plants grown at 30.5°C and exposed to 0.5 mmol l^{-1} Cd in hydroponics possessed thicker cell walls in order to inhibit radial transport and translocation of Cd to shoots and to alleviate induction of oxidative stress and damages to the photosynthetic apparatus. On the other hand, the question arises if Cd uptake and the Cd-induced

damages in *B. decumbens* and *P. maximum* would decrease due to a lower transpiration if these plants were grown at lower temperatures, like they occur in winter?

It is known that the oxidative stress caused by increased levels of reactive oxygen species (ROS) is higher at lower temperatures (Tang et al. 2020), as observed in several forage grasses (Loka et al. 2019), and that oxidative stress should be the primary result of Cd toxicity in plants (Loix et al. 2017). Oxidative stress can cause protein oxidation and lipid peroxidation, which cause the rupture of the plasma membranes and change the structure and numbers of chloroplasts in leaf cells, besides to changes of the water relations and consequently the stomatal conductance and transpiration (Parmar et al. 2013), as observed in *P. maximum* exposed to Cd (Rabêlo et al. 2018d). In order to mitigate the deleterious effects of the oxidative stress, enzymatic and non-enzymatic antioxidants are employed by plants (Soares et al. 2019a). Reduced glutathione (GSH, γ-Glu-Cys-Gly) is the main non-enzymatic antioxidant in plant cells; it can be oxidized to glutathione disulfide (GSSG) in the course of ROS scavenging, which contributes to preventing oxidative damages in the cells (Seth et al. 2012, Jia et al. 2020). Furthermore, GSH is a substrate for synthesis of phytochelatins (PCs) [$(\gamma\text{-Glu-Cys})_n$-Gly, with n = 2-11], i.e. peptides involved in Cd chelation and its transport from the cytosol to the vacuole (Seth et al. 2012). Phytochelatin-mediated Cd storage in the vacuole was reported as an efficient defense strategy in non-hyperaccumulator plants (Jia et al. 2020), as also observed by Santos et al. (2011) in *B. decumbens* and by Rabêlo et al. (2018c) in *P. maximum*. Jia et al. (2018) described that defense mechanisms involved in Cd tolerance in *Pinus sylvestris* were less efficient at ambient compared to higher temperature, despite accumulating more Cd in the roots at the elevated temperature. These authors attributed this result to lower activities of enzymatic antioxidants at ambient temperature.

The most important enzymes involved in antioxidative defense are superoxide dismutases (SOD, EC 1.15.1.1) which dismutate superoxide ($O_2^{\bullet-}$) into hydrogen peroxide (H_2O_2) and H_2O; ascorbate peroxidases (APX, EC 1.11.1.11), catalases (CAT, EC 1.11.1.6) and guaiacol peroxidases (GPX, EC 1.11.1.7) that are involved in reducing H_2O_2 into H_2O; and glutathione reductases (GR, EC 1.6.4.2) which convert GSSG into GSH (Soares et al. 2019a, Szopiński et al. 2019). Although antioxidative enzymes act on ROS scavenging, SODs, CATs, APXs and GPXs apparently are not as important as GSH for mitigating the Cd-induced oxidative stress in *P. maximum* (Rabêlo et al. 2017b, 2018c, 2018d). Therefore, symptoms of oxidative stress in this plant species can be consequence of GSH depletion due to its oxidation, direct Cd binding or its use for synthesis of PCs (Clemens 2006, Jia et al. 2020). Santos et al. (2011) attributed also the Cd-induced oxidative damages of the photosynthetic apparatus of *B. decumbens* to depletion of GSH for synthesis of PCs. Although GSH seems to be more important than antioxidative enzymes to attenuate the Cd-induced oxidative stress in both forage grasses, this relationship is unknown in grasses grown in different season conditions (summer or winter), whilst it is known that the synthesis of antioxidants or/and the activity of the antioxidative enzymes in these plants decreases at lower temperatures (Loka et al. 2019). Therefore, our objectives with this study were: (i) to identify the sites of Cd accumulation in the roots of *B. decumbens* and *P. maximum* and the plant responses developed to prevent Cd translocation from root

to shoot; (ii) to understand how these forage grass species mitigate Cd-induced oxidative stress and protect their photosynthetic apparatus from Cd toxicity; and (iii) to identify whether the mechanisms involved in Cd accumulation and Cd-tolerance are affected by temperature conditions prevailing in summer and winter. Our hypothesis was that in the summer conditions the leaf transpiration should be higher, which would increase Cd translocation from roots to shoot and by consequence more strongly compromise the normal functioning of the photosynthetic apparatus of both grasses in relation to winter conditions. We hypothesized that, also in case of higher Cd uptake (notably in the summer conditions), Cd should be more accumulated in the root apoplast and the action of GSH, PCs and antioxidative enzymes would be larger to avoid damages induced by free Cd ions in either roots and shoots.

Materials and Methods

Soil collection and soil physical-chemical composition

Samples of an Oxisol, classified as Typic Hapludox according to United States Department of Agriculture (USDA 1999), were collected in the most superficial layer (0.0 - 0.2 m depth) in an anthropized area under a native pasture in Piracicaba, state of São Paulo, Brazil (S 22º43'04"; W 47º36'55"). Soil parameters were determined on air-dried soil sieved with a 2-mm mesh: pseudo-total Cd (3051a method; USEPA 2007) = 0.63 mg kg^{-1} soil, pH (0.01 M $CaCl_2$) = 4.8, available phosphorus (P; ion exchange resin) = 22 mg dm^{-3} soil, available sulphur (S; 0.01 mol L^{-1} $Ca(H_2PO_4)_2$) = 3 mg dm^{-3} soil, available potassium (K; ion exchange resin) = 0.1 $mmol_c$ dm^{-3} soil, available calcium (Ca; ion exchange resin) = 3 $mmol_c$ dm^{-3} soil, available magnesium (Mg; ion exchange resin) = 8 $mmol_c$ dm^{-3} soil, available boron (B; hot water) = 0.38 mg dm^{-3} soil, available cooper (Cu; diethylene triamine pentaacetic acid - DTPA at pH 7.3) = 0.7 mg dm^{-3} soil, available iron (Fe; DTPA at pH 7.3) = 46 mg dm^{-3} soil, available manganese (Mn; DTPA at pH 7.3) = 8.9 mg dm^{-3} soil, available zinc (Zn; DTPA at pH 7.3) = 4.2 mg dm^{-3} soil, Al^{3+} (1 M KCl) = 0.5 $mmol_c$ dm^{-3} soil, H+Al (pH SMP) = 15 $mmol_c$ dm^{-3} soil, and soil organic matter (oxidation with 0.4 N $K_2Cr_2O_7$) = 34 g kg^{-1} soil. Granulometric fractions (sand = 828 g kg^{-1} soil, silt = 23 g kg^{-1} soil, and clay = 149 g kg^{-1} soil) were obtained by the hydrometer method (Gee and Bauder 2002).

Plant material and experimental design

The experimental design was a factorial scheme 2 × 2, in which *Brachiaria decumbens* Stapf. cv. Basilisk and *Panicum maximum* Jacq. cv. Massai were grown in two soil conditions (Cd-unpolluted and Cd-polluted Oxisol) and two simulated environmental conditions (summer and winter). The plastic pots used to grow the plants contained 3 kg of Cd-unpolluted soil (0.63 mg kg^{-1}) or Cd-polluted (3.6 mg kg^{-1}) soil. The simulated environmental conditions for summer were: 24 h/30 ± 2ºC, 16/8 h light/dark regime, 220 µmol photons m^{-2} s^{-1} at the leaf level delivered by LED lamps 18W 840 T8C W G, and 75 ± 5% relative humidity; whilst the simulated environmental conditions for winter were: 24 h/22 ± 2ºC, 14/10 h light/dark regime, 220 µmol photons m^{-2} s^{-1}, and 55 ± 5% relative humidity. The

temperatures were defined considering the averages recorded in the last 10 years in the summer and winter of Piracicaba. The plastic pots used to grow the plants were distributed in a completely randomized design with four replicates per condition. It is important to mention that Cd concentrations between 0.01 and 0.8 mg kg^{-1} are considered non-toxic (Kabata-Pendias 2011), while Cd concentrations ≥ 3.6 mg kg^{-1} present direct and indirect potential risks to the human health, according to the guiding values of The Environmental Company of São Paulo - CETESB, in Brazil (CETESB 2014).

Soil pollution, growth conditions, plant harvesting and samples collection

After collection, drying and characterization, the Oxisol was spiked with Cd using $CdCl_2$. At the same day, the basic fertilization was applied following the recommendation for forage grasses (Werner et al. 1997), except for Ca that was applied to increase Ca:Mg ratio in order to avoid Ca deficiency in the two species. Nutrients were applied as pure substances through the nutrient solution. The fertilizer doses consisted of 100 mg N (NH_4NO_3), 100 mg P ($NH_4H_2PO_4$), 150 mg K (KCl), 50 mg S ($ZnSO_4$) and 160 mg Ca ($CaCl_2$) per kg of soil. Subsequently, the soils were incubated for 15 days. After this, seeds of both *B. decumbens* and *P. maximum* were sown. Twenty days later, the seedlings were thinned leaving only 10 seedlings per pot. Between sowing and thinning, all plants were kept at summer condition to accelerate germination. After thinning the plants were exposed to different seasonal conditions. Fifty-four days after seeds germination 100 mg N (NH_4NO_3) and 100 mg K (KCl) per kg of soil were applied (Werner et al. 1997). The soil moisture content was maintained at a constant level (70% of the maximum water holding capacity) during the study in the winter and summer conditions through deionized water supply.

Sixty-three days after sowing, the photosynthetic parameters (described below) were determined on the first fully expanded leaf, and samples of leaves and roots were collected for morpho-anatomical and ultrastructural analyses. One day later, the plants were harvested and separated into shoots and roots. The shoots were separated into leaf blades and another sample comprising stems and sheaths. The plant material collected for biomass determination and elemental analyses was dried in a forced ventilation oven at 60°C for 72 h, while the plant material collected for thiol compounds and enzymatic activities analyses was snap frozen in liquid N and stored at -80°C.

Determinations of biomass production and water content

The fresh weights of leaf blades, stems and sheaths, and roots were determined at the moment of the harvest, while the dry biomass was obtained after weighing the oven-dried samples. The water content was calculated as the average percent difference between fresh weight and the dry weight divided by the fresh weight (Aibibu et al. 2010).

Elemental determination in the plant tissues and nutrients use efficiency calculation

The dried plant tissues (leaf blades, stems and sheaths and roots) were ground in a Wiley type mill (Model 4, Thomas Scientific). Total N concentrations and abundance of the rare stable isotope ^{15}N relative to that of the more abundant ^{14}N ($\delta^{15}N$) were determined through an isotope ratio mass spectrometer (Hydra 20-20, Sercon Ltd.) interfaced to an automatic N analyzer (ANCA-GSL, Sercon Ltd.; Barrie and Prosser 1996), after extraction with 1 mol l^{-1} KCl (1:15, plant tissue:solution, w/v), distillation with MgO and Devarda's alloy and titration with 2.5 mmol l^{-1} H_2SO_4 (Tedesco et al. 1985). To determined concentrations of P, K, Ca, Mg, S, B, Cu, Fe, Mn, Mo, Zn and Cd, tissues were digested in a microwave oven (Model Ethos 1600, Milestone) using a mixture of HNO_3 + H_2O_2 following the United States Environmental Protection Agency - USEPA 3051a method (USEPA 2007). Subsequently, the extracts were analysed by inductively coupled plasma optical emission spectrometry (ICP-OES, iCAP 7000 SERIES, Thermo Fisher Scientific). Blank reagent samples were used during the digestion for quality control. Standard reference material (SRM 1515 - apple leaves) was used to assure the accuracy and precision of the extraction and analytical method. From the elemental concentrations the element contents and the nutrient use efficiencies (NUE) were calculated. Element content was obtained by multiplying the element concentration in the tissue by the dry weight of the respective tissue, while the NUE was calculated as described in the equation 1 (Siddiqi and Glass 1981):

$$NUE\ (g^2\ mg^{-1}) = \left[\frac{(total\ dry\ biomass, g)^2}{total\ nutrient\ content\ in\ the\ plant, mg} \right] \quad (1)$$

Determination of Cd concentrations in the root apoplast and root symplast

Cadmium concentrations in apoplast and symplast were determined using the method reported by Rabêlo et al. (2017a). The roots of the plants were divided into two longitudinal sections with equivalent weights; one of the sections was immersed in a container with 150 ml of "desorption" solution (2 mmol l^{-1} $CuCl_2$, 0.5 mmol l^{-1} $CaCl_2$, and 100 mmol l^{-1} HCl) at 5°C for 30 min and the other one was not immersed. $CaCl_2$ was used to maintain cell wall integrity during Cd desorption, and $CuCl_2$ to release Cd (Cd^{2+}) bound to the root apoplast exchange sites. After the desorption process, the two root sections were washed in deionized water, dried and digested as described above. The Cd concentration in the apoplast was calculated as the total Cd concentration (root part not immersed in the desorption solution) minus Cd concentration in the symplast (root part immersed in the desorption solution). We calculated then Cd partitioning between root apoplast and symplast as the percentage of Cd accumulated in the root apoplast or root symplast in relation to total Cd concentration in the roots.

Morpho-anatomical and ultrastructural analyses of the leaves and roots

For histological characterization, samples of leaves (part closest to petiole) were processed for light and transmission electron microscopy. Fixation was done in a modified Karnovsky solution

(Karnovsky 1965; 2% glutaraldehyde, 2% paraformaldehyde, and 5 mmol l^{-1} $CaCl_2$ in 0.05 mol l^{-1} sodium cacodylate buffer, pH 7.2) for 48 h. Subsequently, the samples were rinsed in cacodylate buffer (0.1 mol l^{-1}) and post fixed in 1% osmium tetroxide in 0.1 mol l^{-1} sodium cacodylate buffer, pH 7.2, at room temperature, for 1 h. Dehydration was performed in a graded acetone series during 48h and finally samples were embedded in Spurr epoxy resin (EMS, Electron Microscopy Sciences). Semithin sections (120-200 nm) were collected on glass slides, stained with toluidine blue (2% in water) for 5 min, rinsed in distilled water, and air-dried. The sections were permanently mounted in Entellan®, observed and documented using an upright light microscope (Axioskop 40 Carl Zeiss). Ultrathin sections of leaves (60-90 nm) were obtained using an ultramicrotome (Porter Blum MT2-Dupont-Sorvall) equipped with diamond knife, collected on copper grids (300 mesh), and stained with uranyl acetate (2.5%), followed by lead citrate (0.1%) (Reynolds 1963). The sections were observed at 80 kV under a transmission electron microscope (JEM1400 JEOL), and the images were digitalized.

Scanning electron microscopy was used to assess the morphology of the vascular cylinder region of roots samples. Small pieces of roots (hair root zone) were fixed in the same modified Karnovsky solution for 24 h and transferred to a 10% glycerol solution for 30 min, and then fractured in liquid N. Post-fixation was done in 1% osmium tetroxide in water for 1 h and 30 min at room temperature. Then, the samples were dehydrated with an increasing acetone series, subjected to critical point drying with liquid CO_2 (Leica EM CPD 300), mounted on metal stubs using carbon conductive tape (Pelco Tabs™, Ted Pella, Inc.), and sputter-coated (Leica EM ACE 600) with gold to thickness of 80 nm. The samples were imaged at JEOL JSM-IT300LV operating at 15 kV electron beam.

Determination of thiol compounds in the leaf blades, stems and sheaths and roots

For analysis of thiol compounds the samples were resuspended in 1 ml 0.1% trifluoroacetic acid (TFA) (w/v) with 6.3 mmol l^{-1} DTPA to allow protein precipitation, and then the suspension was homogenized in a bead mill using the TissueLyser LT (QIAGEN) for cell disruption. The homogenate was centrifuged for 10 min at 9900 *g* and 4°C to pellet precipitated proteins and cell fragments. The resulting supernatant was removed and kept on ice prior to derivatization and thiol analysis (Piotrowska-Niczyporuk et al. 2017). Non-protein thiols were extracted and analysed after derivatisation with monobromobimane by reverse-phase HPLC, according to Huguet et al. (2012). Briefly, 25 mg aliquots of material ground in 0.1% TFA, 6.3 mmol l^{-1} DTPA (pH ≤ 1) and 10 µmol l^{-1} N-acetyl-l-cysteine (internal standard) were filtered and incubated with 280 µmol l^{-1} monobromobimane, 125 mmol l^{-1} N-(2-hydroxyethyl)piperazine-N′-(3-propanesulfonic acid) (HEPPS, pH 8.2) and 4 mmol l^{-1} DTPA (30 min, 45°C, in dark). Subsequently, the thiol compounds were separated on a Nova-Pak C18 analytical column (Waters) at 37°C and eluted with a slightly concave gradient of water and methanol. Fluorescent compounds were identified with Ellman's reagent (Ellman 1959) using a Waters 474 fluorescence detector. The quantification was based on N-acetyl-l-cysteine and GSH standards (0-20 µmol l^{-1}) and corrected for derivatisation efficiency (Huguet et al. 2012).

Hydrogen peroxide and lipid peroxidation measurements

Concentrations of H_2O_2 were determined in leaf blades, stems and sheaths, and roots of the plants as described by Alexieva et al. (2001), with some modifications. Firstly, 0.2 g of frozen samples was macerated in 2 ml of 0.1% (w/v) trichloroacetic acid (TCA) in the presence of 20% (w/w) of polyvinyl polypyrrolidone (PVPP). After complete homogenization, 2 ml of extract was centrifuged at 10 000 *g* for 15 min at 4°C. An aliquot of 0.2 ml was taken from the supernatant and then an aliquot of 0.2 ml of 100 mmol l^{-1} potassium phosphate buffer (pH 7.0) and 0.8 ml of 1 mol l^{-1} potassium iodide was added to the mixture. The solution was left for 1 h in darkness to stabilize the reaction and the readings were made in a spectrophotometer (Genesys 10S UV-VIS, Thermo Fisher Scientific) at 390 nm.

Lipid peroxidation was also determined in the leaf blades, stems and sheaths, and roots of both plant species, of which 2-thiobarbituric acid (TBA) reactive compounds were used to estimate the malondialdehyde (MDA) content as measure of lipid peroxidation (Heath and Packer 1968). The initial procedures for MDA measurements were the same as described for H_2O_2. Following centrifugation, 0.25 ml of sample supernatant was added to 1 ml of 20% (w/v) TCA containing 0.5% TBA. The mixture was placed in a water bath at 95°C for 30 min, and then on ice. After 20 min on ice, the samples were centrifuged at 10 000 *g* for 10 min to separate the residues formed during heating and to clarify the samples. Subsequently, spectrophotometer (Genesys 10S UV-VIS) reading were done at 535 and 600 nm.

Extraction and quantification of proteins in the leaf blades

Leaf blades samples were homogenized with a mortar and pestle in 100 mmol l^{-1} potassium phosphate buffer (pH 7.5; 1 g of leaf blade to 3 ml of buffer) containing 1 mmol l^{-1} ethylenediaminetetraacetic acid (EDTA), 3 mmol l^{-1} dithiothreitol (DTT) and 4% (w/v) PVPP (Azevedo et al. 1998). The resulting homogenate was centrifuged at 10 000 *g* for 30 min at 4°C, and the supernatant was stored at -80°C for determination of the activities of antioxidative enzymes. Total soluble protein concentrations were determined by the method of Bradford (1976), using bovine serum albumin - BSA (Protein Standard, Sigma-Aldrich) as standard.

Determination of the activities antioxidative enzymes in the leaf blades

Total SOD activity was determined as described by Giannopolitis and Ries (1977), adding 15 µl of protein extract to a mixture of 1.5 ml 50 mmol l^{-1} sodium phosphate buffer (pH 7.8) containing 13 mmol l^{-1} methionine, 75 µmol l^{-1} nitroblue tetrazolium (NBT), 0.1 mmol l^{-1} EDTA and 2 µmol l^{-1} riboflavin. The reaction was performed at 25°C in a chamber (covered with aluminum foil) with a fluorescent light of 15 W, and after 5 min of light exposure, the light source was turned off and the blue formazane compound produced by NBT photoreduction was measured spectrophotometrically (Genesys 10S UV-VIS) at 560 nm. The same assay was performed with all reagents (but without protein extract) and time of light exposure to be used as negative control.

Total CAT activity was determined spectrophotometrically following the method described by Kraus et al. (1995), with modifications by Azevedo et al. (1998). The reaction medium was composed of 1 ml of 30 mmol l^{-1} H_2O_2 solution in 100 mmol l^{-1} potassium phosphate buffer (pH 7.5). The reaction started adding 25 µl of plant extract, and CAT activity was determined following the decomposition of H_2O_2 at 10 s intervals for 1 min at 240 nm (Genesys 10S UV-VIS).

Total APX activity was determined spectrophotometrically as described by Nakano and Asada (1981). The reaction medium was composed of 15 µl of sample extract and 80 mmol l^{-1} potassium phosphate buffer solution (pH 7.0) containing 5 mmol l^{-1} ascorbic acid (AsA), 1 mmol l^{-1} EDTA and 1.45 mmol l^{-1} H_2O_2. Absorption was measured for 1 min at 290 nm (Genesys 10S UV-VIS).

The total GPX activity was determined spectrophotometrically as described by Matsuno and Uritani (1972), with modifications by Monteiro et al. (2011). The reaction medium contained 890 µl phosphate-citrate buffer (sodium phosphate dibasic 0.2 mol l^{-1}:citric acid 0.1 mol l^{-1}) pH 5, 10 µl enzyme extract and 50 µl 0.2% guaiacol, which was vortex shaken. Then, 50 µl of 9.8 mmol l^{-1} H_2O_2 was added and incubated at 30ºC for 15 min. The reaction was stopped by cooling in an ice water bath, followed by the addition of 50 µl of 2% sodium metabisulphide solution. The reaction mixture was held for 10 min, and the GPX activity was evaluated by monitoring the absorbance at 450 nm (Genesys 10S UV-VIS).

Total GR activity was determined following the method described by Smith et al. (1988), with modifications by Azevedo et al. (1998). The reaction medium (1 ml) was composed of 1 mmol l^{-1} 5,5′-dithiobis-2-nitrobenzoic acid (DTNB), 1 mmol l^{-1} GSSG, 0.1 mmol l^{-1} nicotinamide adenine dinucleotide phosphate (NADPH) and 50 µl protein in 0.1 mmol l^{-1} potassium phosphate buffer solution (pH 7.5). Absorption was measured for 1 min at 412 nm (Genesys 10S UV-VIS).

Determination of the photosynthetic parameters

Photosynthetic parameters [leaf CO_2 assimilation (A), stomatal conductance (g_s), intracellular CO_2 concentration (C_i) and transpiration (E)] were measured on the first fully expanded leaf, using an infrared gas analyzer (Li-6400, Li-cor Inc.). All parameters were measured at a photosynthetic photon flux density of 2,000 µmol m^{-2} s^{-1}, air CO_2 concentration of 400 ± 20 µmol mol^{-1} and block temperature of 25ºC. Measurements were performed following the procedures recommended by Long and Bernacchi (2003). The instantaneous carboxylation efficiency (k), instantaneous water use efficiency (WUE) and intrinsic water use efficiency (WUE_i) were calculated as described in the equations 2 (Farquhar and Sharkey 1982), 3 and 4 (Wang et al. 2016), respectively. Leaf area was determined in a leaf area integrator model LI 3100 (Li-Cor Inc.). A chlorophyll meter (CFL 1030, Falker) was used to evaluate chlorophyll *a* and *b* and the relative content of chlorophyll (Chl) was calculated as chlorophyll a+b.

$$k = \left(\frac{A}{C_i} \right) \qquad (2)$$

$$\mathrm{WUE} = \left(\frac{A}{E}\right) \quad (3)$$

$$\mathrm{WUE_i} = \left(\frac{A}{g_s}\right) \quad (4)$$

where k is the instantaneous carboxylation efficiency (μmol CO_2 m^{-2} s^{-1} Pa^{-1}), A is the leaf CO_2 assimilation (μmol CO_2 m^{-2} s^{-1}), C_i is the intracellular CO_2 concentration (μmol CO_2 mol^{-1}), WUE is the instantaneous water use efficiency (μmol mol^{-1}), E is the transpiration (mmol H_2O m^{-2} s^{-1}), WUE_i is the intrinsic water use efficiency (μmol mol^{-1}) and g_s is the stomatal conductance (mol H_2O m^{-2} s^{-1}).

Statistical analyses

Both normality and homoscedasticity were checked. All data were submitted to a two-way analysis of variance to detect the effects of the seasons and Cd concentrations, and a post-hoc Tukey test ($P \leq 0.05$) to compare means between seasons within each Cd concentration for each plant species and to compare the means between Cd concentrations within each season for each plant species. Statistical analyses were performed using the Statistical Analysis System v. 9.2 (SAS Institute 2008). The graphs were constructed and plotted with SigmaPlot (version 10.0, Systat Software Inc.). Results were expressed as means ± standard error of the mean.

Results

Shoot biomass production of both grasses were not affected by the experimental conditions

The fresh and dry weights of leaf blades (Fig. 1A,D), stems and sheaths (Fig. 1B,E) of *B. decumbens* and *P. maximum* were not changed by the season or presence of Cd in the soil, which was also the case for the fresh and dry weights of roots of *B. decumbens* (Fig. 1C,F). However, the fresh weight of roots of *P. maximum* grown in winter conditions was higher compared to summer condition, regardless of the presence of Cd in the soil (Fig. 1C). The dry weight of roots of *P. maximum* grown in the Cd-polluted soil was 33% lower compared to the unpolluted soil, in the winter condition (Fig. 1F). Like was the case for weight, there was no effect of the season and/or presence of Cd in the Oxisol on the water content of leaf blades (Fig. 1G), stems and sheaths (Fig. 1H) and roots (Fig. 1I) of *B. decumbens*. However, the water content in the stems and sheaths, and roots of *P. maximum* grown in winter conditions was higher than in summer conditions when the plants were grown in the Cd-polluted (Fig. 1H-I).

Both grasses accumulated more Cd in winter conditions, and in the roots Cd accumulation was higher in root apoplast

Cadmium concentrations and Cd contents in all tissues of both forage grasses cultivated in the unpolluted soil were not affected by the season (Fig. 2). However, when the grasses were grown in the Cd-polluted soil, both presented higher Cd concentrations in their leaf blades (Fig. 2A), stems and sheaths (Fig. 2B) and roots (Fig. 2C) after growing in winter compared to summer conditions. As observed for the plants grown in the unpolluted soil, Cd concentration in all tissues of *B. decumbens* cultivated in the Cd-polluted soil was also not dependent on the season (Fig. 2D-F). On the other hand, the Cd concentrations in the stems and sheaths (Fig. 2E) and roots (Fig. 2F) of *P. maximum* from the Cd-polluted soil were respectively 45 and 121% higher in the winter than the summer conditions. Specifically for the roots, no effect of the season on Cd concentrations in the root apoplast (Fig. 3A) and root symplast (Fig. 3B) of both grass species cultivated in the unpolluted soil was observed. On the other hand, when grown in the Cd-polluted soil, Cd concentration in the apoplast of *B. decumbens* grown in winter conditions was 61% higher than after growing in summer conditions (Fig. 3A). Both grass species presented higher Cd concentrations in their root apoplast (Fig. 3A) and root symplast (Fig. 3B) when cultivated in the Cd-polluted soil. Almost 60 and 70% of Cd in the roots of *B. decumbens* was accumulated in the apoplast when this grass was grown in summer and winter conditions, respectively, regardless of Cd concentration in the soil (Fig. 3C). Cadmium accumulation in the root apoplast of *P. maximum* was more affected by Cd concentrations in the soil than the season conditions used for plant growth. Cadmium accumulated in the root apoplast of *P. maximum* cultivated in the Cd-polluted soil was higher than 60%, regardless of the season (Fig. 3C).

Cd exposure increased root diameter and root cell layers, mainly in summer condition

The root hair zone of the roots of both *B. decumbens* and *P. maximum* grown in the unpolluted soil possessed uniseriate epidermis with evenly sized cells; the cortex consisted of uneven diameter cells, regardless of the season (Fig. 4A,C,E,G,I,K,M,O). The central cylinder of both grasses cultivated in the unpolluted soil had the typical structure for these plant species (see Gomes et al., 2011 and Rabêlo et al., 2018b), regardless of the season (Fig. 4E,G,M,O). However, after growing both species in the Cd-polluted soil, pericycle cells were irregular, and the cambial region contained more cell layers and looked disorganized, regardless of the season (Fig. 4F,H,N,P). The diameter of the vascular cylinder of the roots of both grass species grown in summer conditions in the Cd-polluted soil had a bigger diameter compared to the roots of plants from the unpolluted soil (Fig. S1B). Moreover, the plants grown in the Cd-polluted soil had more root hairs than those from the unpolluted soil, mainly in summer conditions (Fig. 4B,J).

Roots of *B. decumbens* were more susceptible to disordered nutrients uptake and nitrogen metabolism, and *P. maximum* presented lower NUE under Cd-induced stress

In general, the nutrient concentrations in the leaf blades and stems and sheaths of *B. decumbens* (Table 1) showed limited differences in function of the season conditions and Cd concentrations in the soil. Plants grown in the Cd-polluted soil in the winter condition had a lower K concentration and higher

concentrations of Ca in the leaf blades; phosphorous in the stems and sheaths was higher after growth in winter than in summer condition. In contrast to the shoots, nutrients concentrations in the roots of *B. decumbens* showed high variations in function of season conditions and Cd concentration in the soil. Concentrations of N, P, K, Ca, Mg, S and Zn in the roots of this species grown in the Cd-polluted soil were higher after growth in winter than summer conditions. When *B. decumbens* was grown in the summer conditions, the concentrations of P, K, Ca, S, Mn and Zn in the roots of plants grown in the Cd-polluted soil were higher compared to unpolluted soil. On the other hand, when this species was grown in the winter condition the concentrations of N, Cu, Fe and Zn in the roots of the plants grown in the Cd-polluted soil was higher than in the roots of plants from unpolluted soil (Table 1).

As observed in *B. decumbens*, the nutrients concentrations in the leaf blades and stems and sheaths of *P. maximum* (Table 1) showed limited differences in function of the season and Cd concentration in the soil. *P. maximum* cultivated in winter conditions on the Cd-polluted soil contained a lower Cu concentration in the leaf blades and higher concentrations of K and Mg in the stems and sheaths compared to summer condition. In contrast to what was observed in the roots of *B. decumbens*, there was also low variation of nutrients concentrations in the roots of *P. maximum* in function of the Cd concentration in the soil, as well as low variation of nutrients concentrations due to the season in the roots of *P. maximum* cultivated in the Cd-polluted soil. However, the concentrations of K, Cu, Mo and Zn in the roots of this species grown in the unpolluted soil were higher in winter than summer conditions (Table 1). *B. decumbens* showed very high Fe concentrations in its roots (> 3300 mg kg^{-1} DW), regardless of the season or Cd concentration in the soil; this was also the case in *P. maximum* (> 2600 mg kg^{-1} DW). These results indicate the formation of Fe plaques on the roots.

In general, the contents of K and B in leaf blades and roots of *B. decumbens* depend on the season and Cd concentration in the soil (Table S1). Nitrogen metabolism (measured through $\delta^{15}N$; see Robinson 2001) in the stems and sheaths and roots of *B. decumbens* grown in the Cd-polluted soil in the winter condition was also function of the season and Cd concentration in the soil (Fig. S2B-C). However, despite the changes in the concentrations of nutrients and N metabolism in *B. decumbens*, NUE did not depend on the season nor Cd concentration in the soil (Fig. S3). As observed for *B. decumbens*, the nutritional changes (nutrients content) caused by the treatments in *P. maximum* were more pronounced in the leaf blades and roots (Table S1). When grown in the Cd-polluted soil in summer conditions, the latter species contained less P and B in the leaf blades compared to unpolluted soil, which was also observed for Fe and Zn in the leaf blades and N, P, Ca, B, Cu, Fe, Mn, Mo and Zn in the roots of the plants grown in the winter condition. *P. maximum* cultivated in the Cd-polluted soil showed also lower NUE of K, Mg, Mn and Mo compared to the unpolluted soil, in winter condition (Fig. S3C,E,J-K), and lower NUE of K and S in summer condition (Fig. S3C,F).

In general, the synthesis of thiol compounds was higher in the shoot than roots in both grasses

The cysteine concentrations in the leaf blades (Fig. 5A) and stems and sheaths (Fig. 5B) of *B. decumbens* grown in summer and *P. maximum* cultivated in summer and winter conditions were

higher after growing in the Cd-polluted than in the unpolluted soil. After growing in the Cd-polluted soil, both species contained higher concentrations of cysteine in their shoots as well as in the stems and sheaths in the summer condition (Fig. 5A,B). Cysteine concentrations in the roots of *B. decumbens* cultivated in the Cd-polluted soil were similar or lower than after growing in the unpolluted soil (Fig. 5C). Roots of *P. maximum* grown in the summer condition contained lower cysteine concentrations when grown in the Cd-polluted soil, but the opposite was the case for the winter condition (Fig. 5C).

The γ-glutamylcysteine (γ-EC) concentration in the leaf blades of *B. decumbens* grown in the Cd-polluted soil was higher than in plants from the unpolluted soil, regardless of the season (Fig. 5D). However, the opposite was observed in the stems and sheaths of this species kept in winter condition (Fig. 5E). As observed in the leaf blades of *B. decumbens*, the γ-EC concentrations in the leaf blades and stems and sheaths (Figs. 5D-E) of *P. maximum* grown in the Cd-polluted soil was higher in winter than summer conditions. There was no effect neither of the season nor Cd concentration in the soil on γ-EC concentration in the roots of *B. decumbens* (Fig. 5F). On the other hand, the roots of *P. maximum* grown in the Cd-polluted soil in summer condition presented higher γ-EC concentrations.

Regardless of the season, there was no effect of Cd pollution in the soil on GSH concentrations in the leaf blades of *B. decumbens* (Fig. 5G), however, the GSH concentrations increased in the stems and sheaths (Fig. 5H). The GSH concentrations in stems and sheaths of *B. decumbens* were higher after growth in summer than in winter conditions, regardless of Cd concentration in the soil (Fig. 5H), but the opposite was observed in the roots (Fig. 5I). When grown in summer conditions, *P. maximum* grown in the Cd-polluted soil presented lower GSH concentrations in its tissues compared to plants from unpolluted soil, but the opposite was observed for plants from winter conditions (Fig. 5G-I). The GSH concentrations in the leaf blades, stems and sheaths, and roots of *P. maximum* kept in winter condition were respectively 97, 33 and 75% higher compared to summer conditions, when this forage grass was grown in the Cd-polluted soil (Fig. 5G-I).

In general, total PCs concentrations in the leaf blades of both grass species did not differ neither in function of the season nor Cd concentration in the soil (Fig. 5J). Furthermore, regardless of the Cd concentration in the soil, PC_2 and PC_5 concentrations in the leaf blades of *B. decumbens* and PC_3 concentration in the leaf blades of *P. maximum* grown in summer were higher than those from winter conditions; the opposite was observed for PC_5 concentration in *P. maximum* (Fig. 5J, analysis not shown). Total PCs concentrations in the stems and sheaths of *B. decumbens* grown in the summer conditions were higher in plants from the Cd-polluted than from the unpolluted soil; the opposite was observed in *P. maximum* grown in both seasons (Fig. 5K). Both grass species contained higher PCs concentrations in the shoots than in the roots (Fig. 5J-L). Total PCs, PC_2, PC_3 and PC_4 concentrations in the roots of *B. decumbens* grown in both season conditions were higher in plants from the Cd-polluted than from the unpolluted soil, and the concentrations in plants from summer conditions were higher than in those from winter conditions (Fig. 5L). In the roots of *P. maximum*, PCs were only detected in plants from winter conditions, with concentrations higher in the case of unpolluted than

Cd-polluted soil (Fig. 5L). In general, the proportion of longer-chain PCs increased in the order roots < stems and sheats < leaf blades (Fig. 5J-L).

Oxidative stress in the leaf blades of both grasses was higher in summer than winter conditions, but only in *P. maximum* SOD and APX activities were increased

In general, H_2O_2 concentrations in the leaf blades (Fig. 6A), stems and sheaths (Fig. 6B) and roots (Fig. 6C) of *B. decumbens* were not significantly changed by the season or Cd concentration in the soil, which was observed also in the stems and sheaths and roots of *P. maximum* (Fig. 6B,C). On the other hand, H_2O_2 concentrations in the leaf blades of *P. maximum* cultivated in the winter conditions were lower compared to the plants grown in the summer conditions and it was always higher in plants from the unpolluted soil (Fig. 6A). The higher H_2O_2 concentration observed in the leaf blades of *P. maximum* grown in summer condition on the unpolluted soil correlated with higher lipid peroxidation level (Fig. 6D), but based on the soluble protein concentration this did not result in protein oxidation (Fig. S4). Like for the H_2O_2 concentration, lipid peroxidation in the leaf blades of *B. decumbens* (Fig. 6D), and in the stems and sheaths (Fig. 6E) and roots (Fig. 6F) of both species did not differ neither in function of the season nor Cd concentration in the soil. In both species, the H_2O_2 concentrations and lipid peroxidation were the highest in the leaf blades, followed by stems and sheaths and roots, respectively (Fig. 6A-F).

The total activities of SOD (Fig. 7A), APX (Fig. 7C), GPX (Fig. 7D) and GR (Fig. 7E) in the leaf blades of *B. decumbens* did not depend on the Cd concentration in the soil. On the other hand, CAT activity (Fig. 7B) in the leaf blades of *B. decumbens* grown in winter conditions in the Cd-polluted soil were 38% higher. In the leaf blades of *B. decumbens* grown in the Cd-polluted soil only CAT activity (Fig. 7B) was slightly affected by the season (29% higher in winter than summer conditions). Similarly, the total activities of SOD (Fig. 7A), CAT (Fig. 7B), APX (Fig. 7C), GPX (Fig. 7D) and GR (Fig. 7E) in the leaf blades of *P. maximum* grown in winter conditions were not affected by the presence of Cd in the soil. However, the activities of SOD (Fig. 7A) and APX (Fig. 7C) in the leaf blades of *P. maximum* from summer conditions were respectivley 13 and 211% higher; GPX activity was 50% lower in the plants grown in the Cd-polluted soil compared to the plants from the unpolluted soil (Fig. 7D). Only the activities of SOD (Fig. 7A) and APX (Fig. 7C) in the leaf blades of *P. maximum* grown in the Cd-polluted soil were affected by the season (respectively 55 and 185%, higher SOD and APX activities in summer conditions grown plants compared to winter conditions).

Cd exposure changed the leaf cell organelles structure, but there was little effect of Cd on leaf gas exchange and chlorophyll concentration

B. decumbens and *P. maximum* cultivated in the unpolluted soil showed high numbers of chloroplasts containing well-compartmentalized grana and organized thylakoids and low accumulation of starch grains (Fig. 8A,C,E,G,M,O,Q,S), regardless of the season. However, when grown on Cd-polluted soil, both species exhibited: (1) reductions in intercellular spaces and expansion of mesophyll cells, which

was more pronounced in summer than winter conditions (Fig. 8B,D,N,P); (2) increases in the size and number of starch grains, mainly when *B. decumbens* was grown in summer and *P. maximum* in winter conditions (Fig. 8F,H-L,R,T-X); (3) increases in the numbers of mitochondria, vacuoles and peroxisomes, as well as disorganization of the thylakoids with undulating membranes (Fig. 8F,H-L,R,T-X); (4) changes in the chloroplast membrane with manifestation of small vesicles when *B. decumbens* was grown in summer (Fig. 8F,I-J) and *P. maximum* in winter conditions (Fig. 8R,U-V); and (5) increases in the size and numbers of plastoglobules, regardless of the season, the most obvious in *B. decumbens* (Fig. 8F,H-L,R,T-X).

The thickness of the leaf blades of both grass species grown in summer conditions was higher in the plants grown on the Cd-polluted soil compared to unpolluted soil (Fig. 1SA). This was not the case for the leaf area. In contrast, the leaf area of *P. maximum* grown in winter conditions was lower after growing the plants on the Cd-polluted soil (Fig. 9A). In general, leaf gas exchange parameters did not change due to presence of Cd in the soil (Fig. 9B-H). On the other hand, leaf CO_2 assimilation (Fig. 9B), transpiration (Fig. 9E), instantaneous carboxylation efficiency (Fig. 9F), and intrinsic water use efficiency (Fig. 9H) in *B. decumbens* grown in the Cd-polluted soil were higher in summer than winter conditions, while the opposite was observed for the intracellular CO_2 concentration (Fig. 9D) and for the instantaneous water use efficiency (Fig. 9G). Stomatal conductance (Fig. 9C) and intracellular CO_2 concentration (Fig. 9D) of *P. maximum* grown in the Cd-polluted soil was higher in winter than summer conditions, while the instantaneous carboxylation efficiency (Fig. 9F) and intrinsic water use efficiency (Fig. 9H) were higher in summer than winter conditions. In general, presence of Cd in the soil and season did not affect chlorophyll concentrations in both species (Fig. 9I-L).

Discussion

Cd accumulation and plant responses developed to prevent Cd translocation from roots to shoot

In non-tolerant plants, uptake usually leads to inhibition of the biomass production (Aibibu et al. 2010, Andresen et al. 2020). In species belonging to the family Poaceae, the reduction of both leaf area and CO_2 assimilation have been attributed to Cd-induced physiological disturbances (Kaznina and Titov 2014), as also observed by Rabêlo et al. (2018d) in *P. maximum* exposed to 0.1 and 0.5 mmol Cd l^{-1} in hydroponics. Nevertheless, the shoot and root biomass production of *B. decumbens* and the shoot biomass production of *P. maximum* grown in the Cd-polluted Oxisol (Fig. 1A-F) did not decrease, even though Cd concentrations reached up to 50 mg kg^{-1} DW in these tissues (Fig. 2A-C). According to Kaznina and Titov (2014) this should be explained by the fact that leaf area (Fig. 9A) and leaf CO_2 assimilation (Fig. 9B) were not affected due to efficient cellular mechanisms to cope with Cd-induced stress. Although several studies have been conducted with *B. decumbens* and *P. maximum* in hydroponics (Kopittke et al. 2010, Santos et al. 2011, Rabêlo et al. 2017a, 2017b, 2018b, 2018c, 2018d, 2019), the mechanisms of these species to cope with the Cd-stress are still poorly understood (Rabêlo et al. 2018a). Moreover, in soils, Cd is not so easily available as in hydroponic systems (Rabêlo et al. 2020). As the roots are the first in contact with Cd, an important defense mechanism

against Cd-induced stress is associated with the plant capacity to decrease or delay the Cd transport through membranes (from the apoplast to symplast) in the root cells, enabling the activation of intracellular Cd detoxification mechanisms (Wójcik et al. 2005, Rabêlo et al. 2017a, Song et al. 2017, Clemens 2019, Andresen et al. 2020).

After 64 days of growth, both *B. decumbens* and *P. maximum* grown in the Cd-polluted Oxisol contained higher Cd-concentrations in the root apoplast than the root symplast (Fig. 3A-C), corroborating the results obtained by Vázquez et al. (1992), Küpper et al. (2000), Wójcik et al. (2005) and Rabêlo et al. (2017a). This indicates that also in forage grasses, the root cell wall has an important role in the process of Cd retaining from root apoplast to xylem transport (Clemens 2019). Initially, Cd^{2+} ions are adsorbed by the negative charges ($RCOO^-$) on the apoplastic surfaces, and the deposition of suberin and lignin in the cell wall further reduce the Cd transport from root apoplast to xylem (Lux et al. 2011, Song et al. 2017). In this study, both grass species cultivated in the Cd-polluted Oxisol showed higher numbers and diameters of the cell layers of the root cambial region (Fig. 4F,H,N,P). This is similar to what was reported for *Pinus sylvestris* (Schützendübel et al. 2001) and *Raphanus sativus* (Vitória et al. 2003) exposed to Cd in hydroponics. On the other hand, Gomes et al. (2011) reported thickening of exodermis and endodermis in *B. decumbens* cultivated in an Oxisol polluted with Cd, Cu, Pb and Zn. Similarly, in Cd hyperaccumulator plants such as *Noccaea caerulescens* (Vázquez et al. 1992) and *Arabidopsis halleri* (Küpper et al. 2000), the cortical apoplast has been regarded as a primary site for Cd accumulation in the roots. It seems that the redox state in the apoplast and the signaling by GSH and H_2O_2 are involved in the process that determines the sites of suberin and lignin deposition in roots (Loix et al. 2017). Although this process is still unclear, it probably affects Cd and nutrients uptake by plants due to changes of root anatomy (Clemens 2019, Andresen et al. 2020).

The higher numbers of root hairs in both grasses grown in the Cd-polluted Oxisol compared to the unpolluted Oxisol (Fig. 4B,J) suggest that Cd accelerated the maturation of the endodermis (Lux et al. 2011). This maturation process can lead to a reduction of the membrane surface area available for ion uptake (Enstone et al. 2003). The ion uptake is also affected by the strong Cd adsorption on the Donnan's spaces of the root apoplast, which changes the nutrients uptake that flow mainly via apoplastic route (used by most heavy metals; Zare et al. 2018), as we observed for Mn and Zn in the roots of *B. decumbens* grown in the summer condition (Table 1). This is in agreement with Kopittke et al. (2010) who observed lower Mn uptake by the roots of *B. decumbens* exposed to Cd, and Rabêlo and Borgo (2016) that observed lower cationic micronutrients uptake by grasses exposed to Cd. The intensity of Mn deficiency strongly affects the root endodermis suberization and ion homeostasis which is important for plants to cope with Cd-induced stress (Chen et al. 2019, Carvalho et al. 2020). Besides Mn and Zn, the concentrations of P, K, Ca and S in the roots of *B. decumbens* grown in the summer condition were lower on the Cd-polluted soil (Table 1). The lower uptake of nutrients such as P, K and Ca can affect the retaining of Cd in the root apoplast (Clemens 2019). Phosphates [$Cd_3(PO_4)_2$] can precipitate Cd in the cell wall (Van Belleghem et al. 2007), while K and Ca play an

important role in the synthesis of cell walls (Guo et al. 2017). In a different way, lower S concentrations can compromise Cd sequestering in the root symplast through a lowered synthesis of S-containing molecules (mainly PCs), as observed by Van Belleghem et al. (2007) in *A. thaliana* roots. Thus, lower nutrients uptake can decrease the plant capacity to retain Cd in the root apoplast and root symplast, and thus lead to higher Cd translocation from roots to shoot.

Phytochelatins are the primary Cd-chelators in the cytosol of plant cells and are involved in Cd transport from cytosol to vacuole (Seth et al. 2012). Like in some Cd hyperaccumulator plants, Cd storage into vacuoles in non-hyperaccumulator plants is an efficient defense strategy against high Cd concentrations (Seth et al. 2012, Jia et al. 2020). However, we only observed a slight induction of PCs synthesis in the roots of *B. decumbens* and *P. maximum* (Fig. 5L) if compared to PCs concentrations observed in the roots of *B. decumbens* (Santos et al., 2011) and *P. maximum* (Rabêlo et al. 2018c) exposed to Cd for 6 to 9 days in hydroponics. This might be correlated with the lower Cd concentrations in the root symplast compared to root apoplast in both grass species (Fig. 3A-C) and different mechanisms of Cd detoxification during acute (hydroponics) and chronic (soil) Cd stress (Wójcik et al. 2015). Pal et al. (2019) suggested that concentration and composition of PCs (e.g. PC_{2-6}) were related to the cytoplasmic Cd concentration in the roots of *Eichhornia crassipes*. We found that *B. decumbens* roots containing up to 50 mg Cd kg^{-1} DW and *P. maximum* roots containing up to 30 mg Cd kg^{-1} DW (Fig. 2C) synthesized PC_2, PC_3 and PC_4, and PC_2 and PC_3 (Fig. 5L), respectively. Rabêlo et al. (2018c) reported that *P. maximum* roots presenting Cd concentrations ranged from 422 to 1580 mg kg^{-1} DW synthesized PC_2, PC_3, PC_4 and structural variations of PCs, such as desglycine PCs [desGly-PC, $(\gamma\text{-Glu-Cys})_n$], PCs isoforms [cys-PC, Cys-$(Glu\text{-}Cys)_n$-Gly] and homo-PCs [h-PCs; $(\gamma\text{-Glu-Cys})_n$-ß-Ala]. Moreover, the long-term Cd exposure in this study might explain the lower PCs concentrations. Heiss et al. (2003) observed that, after long term exposure to Cd, the phytochelatin synthase (PCS, EC 2.3.2.15) that catalyzes PCs synthesis from GSH was induced in leaf blades but not in roots of *Brassica juncea*. This might also be the case in our study, since the GSH pools in leaf blades (Fig. 5G) and roots (Fig. 5I) were similar, but the PCs concentrations in the leaf blades were higher (Fig. 5J) than in the roots (Fig. 5L). The lower PCs synthesis in the roots, mainly in *P. maximum* grown in winter condition in the Cd-polluted soil, may have resulted in Cd-induced root damages leading to lowered root biomass (Fig. 2F).

Cd-induced oxidative stress and protection of the photosynthetic apparatus from Cd toxicity

Although Cd can induce oxidative stress in plant roots, this process is more harmful in the shoots than in roots of *B. decumbens* and *P. maximum* (Santos et al. 2011, Rabêlo et al. 2018d, 2019). Therefore, a high root-to-shoot translocation of Cd can lead to an increased oxidative stress in the shoots. Cadmium can induce oxidative stress by indirect pathways such as the replacement of redox-active metals in proteins and activation of NADPH oxidases, decreasing the GSH pool due to binding of Cd^{2+} to GSH and PCs synthesis, and disturbing electron transport chains leading to the generation of ROS (Clemens 2006, Loix et al. 2017, Jia et al. 2020). Of different forms of the ROS generated, H_2O_2 imposes severe

oxidative stress due to its higher stability in comparison to other ROS (e.g. $O_2^{\bullet-}$), which can lead to high lipid peroxidation and lowered CO_2 assimilation, since the Calvin cycle-related enzymes are very sensitive to H_2O_2 (Loix et al. 2017, Soares et al. 2019a, Szopiński et al. 2019, Bora et al. 2020, Andresen et al. 2020). In this study we observed that the concentrations of H_2O_2 and MDA were much higher in shoots than roots (Fig. 6), which is in agreement with Rabêlo et al. (2018d). However, no Cd-induced increases of H_2O_2 production were observed in tissues of both grass species (Fig. 6A-C), which is evidenced by the preservation of CO_2 assimilation in the shoots under Cd exposure (Fig. 9B). This might be due to (i) an efficient Cd chelation by thiol-containing compounds, and/or to (ii) an efficient deployment of GSH and antioxidative enzymes for ROS scavenging (Rabêlo et al. 2018a).

A high PCs synthesis was observed in the leaf blades of both grass species (Fig. 5J), which is important to limit the Cd-induced damages in the cells, as reported for *B. juncea* (Heiss et al. 2003) and *E. crassipes* (Pal et al. 2019). However, although PCs contribute to diminishing the cell damages induced by Cd, their synthesis may lead to a depletion of the GSH pools and compromise the capacity of plant cells to cope with oxidative stress (Jia et al. 2020), as observed in case of high Cd exposure (Santos et al. 2011, Rabêlo et al. 2018d). Nevertheless, GSH concentrations in the shoots of both grass species did not decrease due to the Cd pollution in the soil (except for *P. maximum* grown in the summer condition, Fig. 5G-H), as well as the concentrations of cysteine (Fig. 5A-B) and γ-EC (Fig. 5D-E). High cysteine and γ-EC concentrations are essentials for plants to cope with Cd-induced oxidative stress, as observed in *P. sylvestris* (Schützendübel et al. 2001), since both are GSH precursors. Gamma-glutamylcysteine synthetase (γ-ECS, E.C. 6.3.2.2) catalyzes the synthesis of γ-EC from glutamate and cysteine, and subsequently, glutathione synthetase (GS, E.C. 6.3.2.3) catalyzes the synthesis of GSH from γ-EC and glycine (Seth et al. 2012). As GSH is the main non-enzymatic antioxidant in plants, its maintenance is essential for plants to cope with Cd-induced oxidative stress, as also observed in other studies (Santos et al. 2011, Rabêlo et al. 2017b, 2018d, 2019, Pal et al. 2019). Apparently, only when the GSH pool is decreasing in the tissues of grasses (*e.g. P. maximum* grown in the Cd-polluted soil in the summer condition; Fig. 5G-I), antioxidative enzymes such as SOD (Fig. 7A) and APX (Fig. 7C) are employed to scavenge the Cd-induced ROS, which is in agreement with Rabêlo et al. (2018d). On the other hand, when *P. maximum* was exposed to high Cd concentrations, SOD and APX often presented lower activities (Yu et al. 2013, Rabêlo et al. 2018d), which can compromise the protection of the photosynthetic apparatus (Dobrikova and Apostolova 2019, Guo et al. 2019). Differences in the activity of antioxidative enzymes in response to Cd suggest that various other anti-oxidative mechanisms may be functioning when there are no severe Cd-induced damages in the photosynthetic apparatus (Szopiński et al. 2019).

The efficient functioning of the antioxidative system, mainly the AsA-GSH cycle, is very important to protect the photosynthetic apparatus against deleterious Cd effects resulting from increased ROS production (e.g. chlorophyll degradation; Parmar et al. 2013, Bora et al. 2020, Tang et al. 2020). Oxidative stress can cause protein oxidation and lipid peroxidation, leading to disruption of thylakoid membranes and alterations in the structure and amount of grana, which interrupts the

reactions in the photosystem II (PSII) and changes the electrons flow between PSII and PSI (Parmar et al. 2013, Andresen et al. 2020). Indeed, Sousa Leite and Monteiro (2019) reported that Cd exposure resulted in lower quantum yield of PSII (Φ PSII) and electron transport rate (ETR) in the first growth of *P. maximum*. However, in our study chlorophyll concentrations in both grass species grown in the Cd-polluted soil were similar to those in plants from the unpolluted soil (Fig. 9I-L), although both species showed disorders in the chloroplast's membranes (Fig. 8F,X). Despite the disorders in the chloroplast membranes and the increased size and numbers of plastoglobules (Fig. 8F,H-L,R,T-X) being an indication of oxidative stress (Austin et al. 2006), CO_2 assimilation was not affected in plants growing on the Cd-polluted soil (Fig. 9B). Since also the total soluble protein concentration did not change due to Cd-exposure (Fig. S4) it is probable that key enzymes of photosynthesis such as ribulose-1,5-bisphosphate carboxylase/oxygenase (RuBisCO, EC 4.1.1.39) and phosphoenolpyruvate carboxylase (PEPcase, EC 4.1.1.31) were also not affected. Our results are similar to those reported by Per et al. (2017) for *B. juncea* exposed to 0.1 mmol Cd l^{-1}. They attributed the preservation of the CO_2 assimilation to the high GSH pool under Cd-stress. However, the preservation of the CO_2 assimilation by *P. maximum* grown in the Cd-polluted soil in summer condition (Fig. 9B), under lower GSH levels (Fig. 5G), suggests that other mechanisms are acting to protect its photosynthetic apparatus from Cd toxicity. Dobrikova and Apostolova (2019) reported that plants exposed to Cd showed higher CO_2 assimilation (despite photosynthetic damages) if treated with brassinosteroids (BRs - involved in physiological processes via activation of different defense mechanisms). They attributed this to increased activities and related transcript levels of antioxidative enzymes induced by the BRs (Dobrikova and Apostolova 2019). Thus, the higher SOD (Fig. 7A) and APX (Fig. 7C) activities in *P. maximum* grown in the Cd-polluted soil in the summer condition might be associated to this hormone signaling.

Besides the involvement of PCs, GSH and antioxidative enzymes in the protection of the photosynthetic apparatus, a proper nutrient balance (especially Ca, Mg and Fe) in the shoots of both species (Tables 1 and S1) contributed to the maintenance of the CO_2 assimilation under Cd-induced stress (Carvalho et al. 2019, 2020). Plants presenting low Ca concentration can show stomatal closure due to entry of Cd in competition to Ca^{2+} into the guard cells (Perfus-Barbeoch et al. 2002), which results in lower CO_2 conductance and inhibition of photosynthesis (Parmar et al. 2013). Cadmium can also replace Mg^{2+} in chlorophylls *a* and *b* causing chlorophyll degradation and thus chlorosis, mainly in plants with low Mg concentration in the shoots (Gillet et al. 2006). However, both grass species did not present neither stomatal closure (Fig. 9C) nor lower intracellular CO_2 concentrations (Fig. 9D), or lower chlorophyll concentrations (Fig. 9I-L) and chlorosis. The proper functioning of the photosynthetic apparatus of both species can also be associated with the formation of Fe plaques [due to the high Fe concentrations in the Oxisol (Longnecker and Welch 1990)] observed in the roots of both species (Table 1). Formation of iron plaques acts as a Fe source that prevents Cd-induced Fe deficiency (Sebastian and Prasad 2016), preventing disturbances in electron transport chains and chlorosis (Longnecker and Welch 1990). The importance of a proper nutritional balance in the

protection of photosynthesis against Cd-induced damage was demonstrated also in *Solanum lycopersicum* (Carvalho et al. 2019) and *Glycine max* (Andresen et al. 2020). Besides of being essential for plants to cope with Cd-induced stress, a proper nutritional balance is also indispensable for the plants to cope also with other abiotic stresses, such as the unfavorable temperatures or water relations (Soares et al. 2019b).

Mechanisms involved in Cd accumulation and tolerance affected by summer or winter conditions

Different conditions of temperature, humidity or daylight length prevailing in summer and winter influence the growth of plants and their responses to abiotic stresses, including heavy metals (Loka et al. 2019). This is particularly important for Cd, since its uptake by plants is influenced by leaf transpiration (Lux et al. 2011), and conditions that increase the transpiration process, such as higher temperatures, supposedly lead to a higher Cd uptake by plants (Ge et al. 2016). However, only *B. decumbens* grown in the Cd-polluted soil showed higher transpiration in the summer than winter conditions (Fig. 9E), and both species contained higher Cd concentrations in their tissues in winter than summer conditions (Fig. 2A-C). First of all, the low transpiration observed in *P. maximum* grown in the summer conditions (Fig. 9E) is probably associated with a low stomatal conductance (Fig. 9C; Farquhar and Sharkey 1982). Schulze et al. (1973) reported that stomatal closure in plants exposed to higher temperatures resulted from water stress, which apparently occurred in *P. maximum* (Fig. 1H-I and 9H). This assumption will be discussed later.

Besides the effects on the physiological processes involved in Cd uptake, the different conditions of the season influence also Cd bioavailability from the soil (Jia et al. 2018). The bioavailability of Cd in our soil was 34% higher in winter conditions compared to summer conditions (Rabêlo et al. 2020) enabling both grasses to take up more Cd in the winter than the summer conditions (Fig. 2A-C). In contrast, Jia et al. (2018) reported that Cd uptake by *P. sylvestris* cultivated in a Luvisol for 3 years was higher under elevated temperature (+ 2ºC) than in ambient temperature. The higher Cd uptake by plants grown at higher temperatures can be attributed to changes in the lipid composition of plasma membrane and its fluidity, facilitating passive and active Cd flux through the membrane (Pourghasemian et al. 2013).

Although both grass species absorbed more Cd in winter than summer conditions (Fig. 2A-C), it was in summer conditions that Cd more strongly induced an increase in the diameter of the root vascular cylinder (Fig. S1B) and numbers of root hairs (Fig. 4F,N). Poerwanto et al. (1989) reported also that root hairs were found mainly in fibrous roots in *Citrus unshiu*, and that after six months of plant growth the numbers of root hairs were higher at 30ºC than 20ºC. The root respiration increases at higher temperatures, leaving fewer carbohydrates for root growth (Szaniawski 1983). In this scenario, Cd-induced deposition of lignin and suberin in root tissues probably accelerates the root cell maturation and increases the root diameter (Fig. S1B). It is also possible that ethylene is involved in the root responses observed in our study, since ethylene mediated reorientation of cell expansion and

has an important role in root hair development (Le et al. 2004). Moreover, according to Enstone et al. (2003), the endo- and exodermal layers of roots mature earlier in water-stressed plants, which might be the case for *P. maximum* grown in the Cd-polluted soil, since this grass showed lower root water content (Fig. 1I) and higher abundance of root hairs (Fig. 4J,L) in the summer condition. On the other hand, Cd did not increase the diameter of the root vascular cylinder (Fig. S1B) of both grass species grown in winter condition, probably because these plants already showed high diameters in the unpolluted soil. Davidson (1969) suggested that grasses cultivated at lower temperatures develop large roots (high diameter) to compensate for the low specific ion fluxes into the roots in this condition. This assumption becomes clear when we observe that *B. decumbens* grown in both Cd-polluted and unpolluted soil showed higher root nutritional disorders in the winter than summer conditions (Table 1). The negative $\delta^{15}N$ observed in the roots of *B. decumbens* grown in the Cd-polluted soil in the winter conditions (Fig. S2C) indicates that nitrate (NO_3^-) and ammonium (NH_4^+) uptake and their metabolism were altered in comparison to the other conditions assayed (Robinson 2001), with N concentrations even increasing in this condition (Table 1). It's noteworthy that changes of the NO_3^-/NH_4^+ metabolism and their proportion can compromise the capacity of grasses to cope with Cd-induced oxidative stress, as observed in *P. maximum* exposed for 4 days to 0.5 or 1 mmol Cd l^{-1} in hydroponics (Sousa Leite and Monteiro 2019).

Changes in the cell wall of root cells, caused by water stress (*P. maximum*) or nutritional disorders (*B. decumbens*) induced by Cd exposure and/or seasonal conditions, affect Cd partitioning in the root apoplast and symplast (Fig. 3C), and in turn, synthesis of thiol compounds involved in intracellular ROS scavenging and Cd chelation (Pourghasemian et al. 2013, Loix et al. 2017). In this study, GSH concentrations in the roots (Fig. 5I) and leaf blades (Fig. 5G) of both grass species cultivated in the Cd-polluted soil were higher in winter than summer conditions, just like the concentrations of Cd in the tissues (Fig. 2A,C). Xu et al. (2006) also reported higher GSH synthesis in the leaf blades of two grass species (*Festuca arundinacea* and *Lolium perenne*) grown at 22ºC compared to 38 or 42ºC using similar conditions to ours (14/10 h light/dark regime, 160 µmol m^{-2} s^{-1} PAR, and 70 ± 10% relative humidity), and attributed this to absence of heat stress. Moreover, in our study the higher GSH concentrations in the winter conditions can be attributed also to higher Cd tissue concentrations observed in this season, since GSH synthesis is strongly Cd-induced (Seth et al. 2012). Also, Repkina et al. (2019) observed higher GSH synthesis in leaf blades of *Triticum aestivum* grown at 4ºC exposed to Cd than in plants grown at 4ºC without Cd exposure. According to these authors, the higher GSH synthesis in the leaf blades of plants exposed to Cd decreased the lipid peroxidation in the tissue, as we also observed in our study (Fig. 6D). It seems obvious that GSH plays an essential role to attenuate Cd-induced oxidative stress in conditions of lower temperatures in both grass species, since Cd chelation through PCs (Fig. 5J-L) and ROS scavenging by SOD, CAT, APX and GPX (Fig. 7A-D) were not induced (except CAT activity in *B. decumbens*) when the plants were grown in the winter condition on the Cd-polluted soil. In this way, the higher oxidative stress induced at lower temperatures (Tang et al. 2020) in several grasses (Loka et al. 2019) may be associated to lower GSH

pools. This assumption seems to be also valid for high temperatures, since the leaf blades of both grasses grown in the summer conditions presented lower GSH concentrations (Fig. 5G) and higher lipid peroxidation (Fig. 6D). A lower GSH pool in grasses grown at higher temperatures often results in oxidative stress and severe damages to chloroplasts (Xu et al. 2006).

The Cd-induced reduction in intercellular spaces and expansion of mesophyll cells in the leaf blades were stronger in plants grown in summer than winter conditions, mainly in *P. maximum* (Fig. 8B,D,N,P). This is a common response in plants exposed to water stress (Utrillas and Alegre, 1997). Both higher temperatures and Cd exposure can induce water stress (Schulze et al. 1973, Clemens 2006). Thus, the combination of both factors apparently resulted in water stress in *P. maximum*, since this grass contained lower water contents in roots and stems and sheaths (Fig. 1H-I), and higher WUE_i (Fig. 9H) when grown in the Cd-polluted soil in the summer conditions. Gago et al. (2014) detailed that higher WUE_i occurs due to stomatal closure (Fig. 9C) in order to avoid water loss under water deficit conditions. Besides the changes in the mesophyll cells, *B. decumbens* showed also increases in the size and numbers of starch grains and changes in the chloroplasts membrane when grown in the summer condition (Fig. 8F,H-L). However, *P. maximum* presented these changes mainly in the winter conditions (Fig. 8R,T-X). The starch grain accumulation in the chloroplasts of *B. decumbens* grown in the summer conditions may be associated with the conservation of sucrose synthesis under high temperature as well as greater carbon fixation (Bita and Gerats 2013), since this grass showed high carboxylation (Fig. 9F) and CO_2 assimilation (Fig. 9B) in summer conditions. Rabêlo et al. (2018c,d) reported that sucrose synthesis in the leaf blades of *P. maximum* grown at 30.5ºC was maintained under Cd exposure enabling carbon fixation and preservation of photosynthetic rate. On the other hand, Pietrini et al. (2003) mentioned that high intracellular CO_2 concentrations (Fig. 9D) in plants exposed to Cd at lower temperature can lead to accumulation of starch grains (as observed in *P. maximum*) as a result of a limiting phosphate recycling between cytosol and chloroplasts caused by a lower sucrose synthesis induced by Cd. In turn, the higher intracellular CO_2 concentrations observed in *P. maximum* grown in the winter condition (Fig. 9D) can be associated with inhibition of RuBisCO activity, which results in lower CO_2 carboxylation (Fig. 9F; Wang et al. 2016). According to Bita and Gerats (2013) the seasonal effects on the photosynthesis process strongly vary between different species, mainly when there is interaction with other factors. Therefore, further studies are necessary to better understand the interactions between influence of the season and Cd stress on C_4 photosynthesis of grasses, since there are other aspects involved in effective photosynthetic adaptation at different temperature and water conditions.

Conclusion

The main site of Cd accumulation in the roots of both *B. decumbens* and *P. maximum* was the apoplast, but Cd partitioning between root apoplast and symplast can be affected by seasonal variations that induced nutritional disorders in *B. decumbens* grown in winter and water stress in *P. maximum* grown in summer conditions. Both nutritional disorders and water stress in these grass

species probably affect cell wall composition and the Cd-induced root cell maturation. However, specific studies are necessary to examine this assumption. Although the root apoplast had an important role in Cd retention in the roots of both grass species, it was not sufficiently effective to prevent Cd translocation from roots to shoots in *B. decumbens* and *P. maximum*.

The high roots to shoots translocation of Cd resulted in higher oxidative stress in the shoots than roots in both grass species, but the shoot biomass production did not decrease due to the high Cd concentrations. Therefore, this indicates that the photosynthetic apparatus of both species was protected from oxidative stress induced by Cd and seasonal variations. This protection was provided by both PCs, that act as Cd chelators, and by GSH that limited lipid peroxidation. GSH levels seem to be more important than SOD, CAT, APX and GPX activities to attenuate the oxidative stress in the leaf blades. These enzymes seem to act as a secondary protection mechanism and were mobilized only when the GSH pool was low. Moreover, a proper nutrient balance in the shoots of both species enabled an appropriate photosynthetic activity. On the other hand, the preservation of photosynthesis in *P. maximum* under water stress in summer condition suggests that other factors are involved in effective protection of the photosynthetic apparatus from the stress induced by Cd and/or seasonal variations, such as phytohormones or antioxidants that act as osmolytes. This should be investigated in more details in further studies.

Author contributions

F.H.S.R. performed the experiment and drafted the manuscript. S.A.G. performed the analyses involving the antioxidant enzymes. M.L.R. performed the anatomical and ultrastructural analyses. N.M.S. measured the photosynthetic parameters while M.W., A.B. and A.P. measured the thiol compounds. N.M.S., M.W., A.B., A.P., F.S.L., R.A.A. and J.V. contributed to interpretation of results. L.R.F.A. coordinated the study. All authors contributed to critical review of manuscript and approved its final version.

Acknowledgments - This study was supported by São Paulo Research Foundation - FAPESP (grants #2017/11299-8 and #2018/07190-3) and by the Hasselt University Methusalem project 08M03VGRJ. The authors thank the Profs Francisco José Krug, José Albertino Bendassolli and Paulo Cesar Ocheuze Trivelin, the lab technicians Aparecida de Fátima Patreze and Liz Mary Bueno de Moraes, and the master Nicolas Braga Casarin from CENA/USP for their contribution in the nutritional and $\delta^{15}N$ isotopic analyses; and Rodrigo Hideki Mano from ESALQ/USP for his contribution in the study conduction. We also thank to Centro de Microscopia e Imagem (FOP/UNICAMP) and NAP/MEPA (ESALQ/USP) for the access to Transmission and Scanning electron microscopies, respectively. Ricardo Antunes Azevedo thanks Conselho Nacional de Desenvolvimento Científico e Tecnológico - CNPq (grant #303749/2016-4) for the research fellowship.

Data availability statement

The data that support the findings of this study are available from the corresponding author upon reasonable request.

References

Aibibu N, Liu Y, Zeng G, Wang X, Chen B, Song H, Xu L (2010) Cadmium accumulation in *vetiveria zizanioides* and its effects on growth, physiological and biochemical characters. Bioresour Technol 101: 6297-6303

Alexieva V, Sergiev I, Mapelli S, Karanov E (2001) The effect of drought and ultravioleta radiation on growth and stress markers in pea and wheat. Plant Cell Environ 24: 1337-1344

Andresen E, Lyubenova L, Hubáček T, Bokhari SNH, Matoušková Š, Mijovilovich A, Rohovec J, Küpper H (2020) Chronic exposure of soybean plants to nanomolar cadmium reveals specific additional high-affinity targets of cadmium. J Exp Bot 71: 1628-1644

Austin JR, Frost E, Vidi PA, Kessler F, Staehelin LA (2006) Plastoglobules are lipoprotein subcompartments of the chloroplast that are permanently coupled to thylakoid membranes and contains biosynthetic enzymes. Plant Cell 18: 1693-1703

Azevedo RA, Alas RM, Smith RJ, Lea PJ (1998) Response of antioxidant enzymes to transfer from elevated carbon dioxide to air and ozone fumigation, in the leaves and roots of wild-type and a catalase-deficient mutant of barley. Physiol Plant 104: 280-292

Barrie A, Prosser SJ (1996) Automated analysis of light-element stable isotopes by isotope ratio mass spectrometry. In: Boutton TW, Yamasaki S (eds) Mass Spectrometry of Soils. Marcel Dekker, New York, pp 1-46

Bita CE, Gerats T (2013) Plant tolerance to high temperature in a changing environment: scientific fundamentals and production of heat stress-tolerant crops. Front Plant Sci 4: 273

Bora MS, Gogoi N, Asrma KP (2020) Tolerance mechanism of cadmium in *Ceratopteris pteridoides*: Translocation and subcellular distribution. Ecotox Environ Safe 197: 110599

Bradford MM (1976) A rapid and sensitive method for the quantification of microgram quantities of protein utilizing principle of protein-dye-binding. Anal Biochem 72: 248-254

Carvalho ME, Piotto FA, Franco MR, Rossi ML, Martinelli AP, Cuypers A, Azevedo RA (2019) Relationship between Mg, B and Mn status and tomato tolerance against Cd toxicity. J Environ Manage 240: 84-92

Carvalho MEA, Castro PRC, Kozak M, Azevedo RA (2020) The sweet side of misbalanced nutrients in cadmium-stressed plants. Ann Appl Biol 176: 275-284

CETESB - The Environmental Company of São Paulo (2014) Guiding values for soil and groundwater in the State of São Paulo. Available at https://cetesb.sp.gov.br/solo/wp-content/uploads/sites/18/2014/12/valores-orientadores-nov-2014.pdf (In Portuguese)

Chen A, Husted S, Salt DE, Schjoerring JK, Persson DP (2019) The intensity of manganese deficiency strongly affects root endodermal suberization and ion homeostasis. Plant Physiol 181: 729-742

Clemens S (2006) Toxic metal accumulation, responses to exposure and mechanisms of tolerance in plants. Biochimie 88: 1707-1719

Clemens S (2019) Safer food through plant science: reducing toxic element accumulation in crops. J Exp Bot 70: 5537-5557

Davidson RL (1969) Effect of root/leaf temperature differentials on root/shoot ratios in some pasture grasses and clover. Ann Bot 33: 561-569

Dobrikova AG, Apostolova EL (2019) Damage and protection of the photosynthetic apparatus under cadmium stress. In: Hasanuzzaman M, Prasad MNV, Fujita M (eds) Cadmium toxicity and tolerance in plants, 1st Edn. Elsevier, London, pp 275-298

Ellman G (1959) Tissue sulfhydryl groups. Arch Biochem Biophys 82: 70-77

Enstone DE, Peterson CA, Ma F (2003) Root endodermis and exodermis: Structure, function, and responses to the environment. J Plant Growth Regul 21: 335-351

Farquhar GD, Sharkey TD (1982) Stomatal conductance and photosynthesis. Annu Rev Plant Physiol 33: 317-345

Gago J, Douthe C, Florez-Sarasa I, Escalona JM, Galmes J, Fernie AR, Flexas J, Medrano H (2014) Opportunities for improving leaf water use efficiency under climate change conditions. Plant Sci 226: 108-119

Ge L, Cang L, Yang J, Zhou D (2016) Effects of root morphology and leaf transpiration on Cd uptake and translocation in rice under different growth temperature. Environ Sci Pollut Res 23: 24205-24214

Gee GW, Bauder J (2002) Particle-size analysis. In: Dane JH, Toop GC (eds) Methods of soils analysis. Part 4: Physical methods. Soil Science Society of America, Madison, pp 255-293

Giannopolitis CN, Ries SK (1977) Superoxide dismutases. Plant Physiol 59: 309-314

Gillet S, Decottignies P, Chardonnet S, Le Maréchal P (2006) Cadmium response and redoxin targets in *Chlamydomonas reinhardtii*: a proteomic approach. Photosynth Res 89: 201-211

Gomes MP, Marques TCLLDM, Nogueira MDG, de Castro EM, Soares AM (2011) Ecophysiological and anatomical changes due to uptake and accumulation of heavy metal in *Brachiaria decumbens*. Sci Agric 68: 566-573

Guo K, Tu L, He Y, Deng J, Wang M, Huang H, Li Z, Zhang X (2017) Interaction between calcium and potassium modulates elongation rate in cotton fiber cells. J Exp Bot 68: 5161-5175

Guo J, Qin S, Rengel Z, Gao W, Nie Z, Liu H, Li C, Zhao P (2019) Cadmium stress increases antioxidant enzyme activities and decreases endogenous hormone concentrations more in Cd-tolerant than Cd-sensitive wheat varieties. Ecotox Environ Safe 172: 380-387

Heath RL, Packer L (1968) Photoperoxidation in isolated chloroplasts. I. Kinetics and stoichiometry of fatty acid peroxidation. Arch Biochem Biophys 125: 189-198

Heiss S, Wachter A, Bogs J, Cobbett C, Rausch T (2003) Phytochelatin synthase (PCS) protein is induced in *Brassica juncea* leaves after prolonged Cd exposure. J Exp Bot 54: 1833-1839

Huguet S, Bert V, Laboudigue A, Barthès V, Isaure M-P, Llorens I, Schat H, Sarret G (2012) Cd speciation and localization in the hyperaccumulator *Arabidopsis halleri*. Environ Exp Bot 82: 54-65

Jia X, Liu T, Li X, Zhao Y (2018) Needles resistance in *Pinus sylvestris* L. var. mongolica Litv. exposed to elevated air temperature and cadmium-contaminated soils for 3 years. Water Air Soil Pollut 229: 188

Jia H, Hou D, O'comnor D, Pan S, Zhu J, Bolan NS, Umlder J (2020) Exogenous phosphorus treatment facilitates chelation-mediated cadmium detoxification in perennial ryegrass (*Lolium perenne* L.). J Hazard Mater 389: 121849

Kabata-Pendias A (2011) Trace elements in soils and plants. 4th Edn. CRC Press, Boca Raton

Karnovsky MJ (1965) A formaldehyde-glutaraldehyde fixative of high osmolality for use in electron microscopy. J Cell Biol 27: 137-138

Kaznina NM, Titov AF (2014) The influence of cadmium on physiological processes and productivity of Poaceae plants. Biol Bull Rev 4: 335-348

Kopittke PM, Blamey FPC, Menzies NW (2010) Toxicity of Cd to signal grass (*Brachiaria decumbens* Stapf.) and Rhodes grass (*Chloris gayana* Kunth.). Plant Soil 330: 515-523

Kraus TE, McKersie BD, Fletcher RA (1995) Paclobutrazol-induced tolerance of wheat leaves to paraquat may involve increased antioxidant enzyme activity. J Plant Physiol 145: 570-576

Küpper H, Lombi E, Zhao F-J, McGrath SP (2000) Cellular compartmentation of cadmium and zinc in relation to other elements in the hyperaccumulator *Arabidopsis halleri*. Planta 212: 75-84

Le J, Vandenbussche F, Van Der Straeten D, Verbelen J (2004) Position and cell type-dependent microtubule reorientation characterizes the early response of the Arabidopsis root epidermis to ethylene. Physiol Plant 121: 513-519

Loix C, Huybrechts M, Vangronsveld J, Gielen M, Keunen E, Cuypers A (2017) Reciprocal interactions between cadmium-induced cell wall responses and oxidative stress in plants. Front Plant Sci 8: 1867

Loka D, Harper J, Humphreys M, Gasior D, Wootton-Beard P, Gwynn-Jones D, Scullion J, Doonan J, Kingston-Smith A, Dodd R, Wang J, Chadwick D, Hill P, Jones D, Mills G, Hayes F, Robinson D (2019). Impacts of abiotic stresses on the physiology and metabolism of cool-season grasses: A review. Food Energy Secur 8: e00152

Long SP, Bernacchi CJ (2003) Gas exchange measurements, what can they tell us about the underlying limitations to photosynthesis? Procedures and sources of error. J Exp Bot 4: 2393-2401

Longnecker N, Welch RM (1990) Accumulation of apoplastic iron in plant roots: a factor in the resistance of soybeans to iron-deficiency induced chlorosis? Plant Physiol 92: 17-22

Lux A, Martinka M, Vaculík M, White PJ (2011) Root responses to cadmium in the rhizosphere: a review. J Exp Bot 62: 21-37

Matsuno H, Uritani I (1972) Physiological behavior of peroxidase isozymes in sweet potato root tissue injured by cutting or with black rot. Plant Cell Physiol 13: 1091-1101

Monteiro CC, Carvalho RF, Gratão PL, Carvalho G, Tezotto T, Medici LO, Peres LEP, Azevedo RA (2011) Biochemical responses of the ethylene-insensitive *Never ripe* tomato mutant subjected to cadmium and sodium stresses. Environ Exp Bot 71: 306-320

Nakano Y, Asada K (1981) Hydrogen peroxide is scavenged by ascorbate-specific peroxidase in spinach chloroplasts. Plant Cell Physiol 22: 867-880

Pal R, Kaur R, Rajwar D, Rai JPN (2019) Induction of non-protein thiols and phytochelatins by cadmium in *Eichhornia crassipes*. Int J Phytoremediat 21: 790-798

Parmar P, Kumari N, Sharma V (2013) Structural and functional alterations in photosynthetic apparatus of plants under cadmium stress. Bot Stud 54: 45

Per TS, Masood A, Khan NA (2017) Nitric oxide improves S-assimilation and GSH production to prevent inhibitory effects of cadmium stress on photosynthesis in mustard (*Brassica juncea* L.). Nitric Oxide 68: 111-124

Perfus-Barbeoch L, Leonhardt N, Vavasseur A, Forestier C (2002) Heavy metal toxicity: cadmium permeates through calcium channels and disturbs the plant water status. Plant J 32: 539-548

Pietrini F, Iannelli MA, Pasqualini S, Massacci A (2003) Interaction of cadmium with glutathione and photosynthesis in developing leaves and chloroplasts of *Phragmites australis* (Cav.) Trin. ex Steudel. Plant Physiol 133: 829-837

Piotrowska-Niczyporuk A, Bajguz A, Zambrzycka-Szelewa E (2017) Response and the detoxification strategies of green alga *Acutodesmus obliquus* (Chlorophyceae) under lead stress. Environ Exp Bot 144: 25-36

Poerwanto R, Inoue H, Kataoka I (1989) Effects of temperature on the morphology and physiology of the roots of trifoliate orange budded with Satsuma Mandarin. J Japan Soc Hort Sci 58: 267-274

Pourghasemian N, Ehsanzadeh P, Greger M (2013) Genotypic variation in safflower (*Carthamus* spp.) cadmium accumulation and tolerance affected by temperature and cadmium levels. Environ Exp Bot 87: 218-226

Rabêlo FHS, Borgo L (2016) Changes caused by heavy metals in micronutrient content and antioxidant system of forage grasses used for phytoremediation: an overview. Cienc Rural 46: 1368-1375

Rabêlo FHS, Jordão LT, Lavres J (2017a) A glimpse into the symplastic and apoplastic Cd uptake by Massai grass modulated by sulfur nutrition: plants well-nourished with S as a strategy for phytoextraction. Plant Physiol Biochem 121: 48-57

Rabêlo FHS, Azevedo RA, Monteiro FA (2017b) Proper supply of S increases GSH synthesis in the establishment and reduces tiller mortality during the regrowth of Tanzania guinea grass used for Cd phytoextraction. J Soils Sediments 17: 1427-1436

Rabêlo FHS, Azevedo RA, Monteiro FA (2017c) The proper supply of S increases amino acid synthesis and antioxidant enzyme activity in Tanzania guinea grass used for Cd phytoextraction. Water Air Soil Pollut 228: 394

Rabêlo FHS, Borgo L, Lavres J (2018a) The use of forage grasses for the phytoremediation of heavy metals: plant tolerance mechanisms, classifications, and new prospects. In: Matichenkov V (ed) Phytoremediation: Methods, Management and Assessment. Nova Science Publishers, New York, pp 59-103

Rabêlo FHS, Lux A, Rossi ML, Martinelli AP, Cuypers A, Lavres J (2018b) Adequate S supply reduces the damage of high Cd exposure in roots and increases N, S and Mn uptake by Massai grass grown in hydroponics. Environ Exp Bot 148: 35-46

Rabêlo FHS, Fernie AR, Navazas A, Borgo L, Keunen E, Silva BKA, Cuypers A, Lavres J (2018c) A glimpse into the effect of sulfur supply on metabolite profiling, glutathione and phytochelatins in *Panicum maximum* cv. Massai exposed to cadmium. Environ Exp Bot 151: 76-88

Rabêlo FHS, Silva, BKA, Borgo L, Keunen E, Rossi ML, Borges KLR, Santos EF, Reis AR, Martinelli AP, Azevedo RA, Cuypers A, Lavres J (2018d) Enzymatic antioxidants - relevant or not to protect the photosynthetic system against cadmium-induced stress in Massai grass supplied with sulfur? Environ Exp Bot 155: 702-717

Rabêlo FHS, Moral RA, Lavres J (2019) Integrating biochemical, morpho-physiological, nutritional and productive responses to Cd accumulation in Massai grass employed in phytoremediation. Water Air Soil Pollut 230: 110

Rabêlo FHS, Borgo L, Merloti LF, Pylro VS, Navarrete AA, Mano RH, Thijs S, Vangronsveld J, Alleoni LRF (2020) Effects of winter and summer conditions on Cd fractionation and bioavailability, bacterial communities and Cd phytoextraction potential of *Brachiaria decumbens* and *Panicum maximum* grown in a tropical soil. Sci Total Environ 728: 138885

Repkina N, Talanova V, Ignatenko A, Titov A (2019) Involvement of proline and non-protein thiols in response to low temperature and cadmium stresses in wheat. Biol Plant 63: 70-77

Reynolds ES (1963) The use of lead citrate at high pH as an electron-opaque stain in electron microscopy. J Cell Biol 17: 208-212

Robinson D (2001) $\delta^{15}N$ as an integrator of the nitrogen cycle. Trends Ecol Evol 16: 153-162

Santos FS, Amaral Sobrinho NMB, Mazur N, Garbisu C, Barrutia O, Becerril JM (2011) Antioxidant response, phytochelatins formation and photoprotective pigment composition in *Brachiaria decumbens* Stapf subjected to contamination with Cd and Zn. Quim Nova 34: 16-20

SAS Institute (2008) SAS User's guide: Statistics. Version 9.2. Available at http://support.sas.com/software/92/ (accessed 26 Feb 2019)

Schulze ED, Lange OL, Kappen L, Buschbom U (1973) Stomatal responses to changes in temperature at increasing water stress. Planta 110: 29-42

Schützendübel A, Schwanz P, Teichmann T, Gross K, Langenfeld-Heyser R, Godbold DL, Polle A (2001) Cadmium-induced changes in antioxidative systems, hydrogen peroxide content and differentiation in Scots pine roots. Plant Physiol 127: 887-898

Sebastian A, Prasad MNV (2016) Iron plaque decreases cadmium accumulation in *Oryza sativa* L. and serves as a source of iron. Plant Biol 18: 1008-1015

Seth CS, Remans T, Keunen E, Jozefczak M, Gielen H, Opdenakker K, Weyens N, Vangronsveld J, Cuypers A (2012) Phytoextraction of toxic metals: a central role for glutathione. Plant Cell Environ 35: 334-346

Siddiqi MY, Glass ADM (1981) Utilization index: a modified approach to the estimation and comparison of nutrient utilization efficiency in plants. J Plant Nutr 4: 289-302

Smith IK, Vierheller TL, Thorne CA (1988) Assay of glutathione reductase in crude tissue homogenates using 5,5'-dithilbis (2-nitrobenzoic acid). Anal Biochem 175: 408-413

Soares C, Carvalho MEA, Azevedo RA, Fidalgo F (2019a) Plants facing oxidative challenges - a little help from the antioxidant networks. Environ Exp Bot 161: 4-25

Soares JC, Santos CS, Carvalho SMP, Pintato MM, Vasconcelos MW (2019b) Preserving the nutritional quality of crop plants under a changing climate: importance and strategies. Plant Soil 443: 1-26

Song Y, Jin L, Wang X (2017) Cadmium absorption and transportation pathways in plants. Int J Phytoremediat 19: 133-141

Sousa Leite T, Monteiro FA (2019) Partial replacement of nitrate by ammonium increases photosynthesis and reduces oxidative stress in tanzania guinea grass exposed to cadmium. Ecotox Environ Safe 174: 592-600

Szopiński M, Sitko K, Gieroń Ż, Rusinowski S, Corso M, Hermans C, Verbruggen N, Małkowski E (2019) Toxic Effects of Cd and Zn on the Photosynthetic Apparatus of the *Arabidopsis halleri* and *Arabidopsis arenosa* Pseudo-Metallophytes. Front Plant Sci 10: 748

Suman J, Uhlik O, Viktorova J, Macek T (2018) Phytoextraction of heavy metals: a promising tool for clean-up of polluted environment? Front Plant Sci 9: 1476

Szaniawski RK (1983) Adaptation and functional balance between shoot and root activity of sunflower plants grown at different root temperatures. Ann Bot 51: 453-459

Tang X, An B, Cao D, Xu R, Wang S, Zhang Z, Liu X, Sun X (2020) Improving photosynthetic capacity, alleviating photosynthetic inhibition and oxidative stress under low temperature stress with exogenous hydrogen sulfide in Blueberry Seedlings. Front Plant Sci 11: 108

Tedesco MJ, Volkweiss SJ, Bohnen H (1985) Analysis of soil, plants and other materials. Federal University of Rio Grande do Sul, Porto Alegre (In Portuguese)

USDA - United States Department of Agriculture (1999) Soil taxonomy: a basic system of soil classification for making and interpreting soil surveys. U.S. Government Printing Office, Washington

USEPA - United States Environmental Protection Agency (2007) Method 3051A (SW-846): Microwave Assisted Acid Digestion of Sediments, Sludges, and Oils," Revision 1. Washington, DC

Utrillas MJ, Alegre L (1997) Impact of water stress on leaf anatomy and ultrastructure in *Cynodon dactylon* (L.) Pers. under natural conditions. Int J Plant Sci 158: 313-324

Van Belleghem F, Cuypers A, Semane B, Smeets K, Vangronsveld J, D'Haen J, Valcke R (2007) Subcellular localization of cadmium in roots and leaves of *Arabidopsis thaliana*. New Phytol 173: 495-508

Vázquez MD, Barceló J, Poschenrieder Ch, Mádico J, Hatton P, Baker AJM, Cope GH (1992) Localization of zinc and cadmium in *Thlaspi caerulescens* (*Brassicaceae*), a metallophyte that can accumulate both metals. J Plant Physiol 140: 350-355

Vitória AP, Rodriguez APM, Cunha M, Lea PJ, Azevedo RA (2003) Structural changes in radish seedlings exposed to cadmium. Biol Plant 47: 561-568

Wang X, Wang L, Shangguan Z (2016) Leaf gas exchange and fluorescence of two winter wheat varieties in response to drought stress and nitrogen supply. PLoS ONE 11: e0165733

Werner JC, Paulino VT, Cantarella H, Andrade NO, Quaggio JA (1997) Forages. In: Raij B van, Cantarella H, Quaggio JA, Furlani AMC (eds) Fertilization and liming recommendations for the State of São Paulo. IAC, Campinas pp 263-273 (In Portuguese)

Wójcik M, Vangronsveld J, D'Haen J, Tukiendorf A (2005) Cadmium tolerance in *Thlaspi caerulescens* II. Localization of cadmium in *Thlaspi caerulescens*. Environ Exp Bot 53: 163-171

Wójcik M, Dresler S, Tukiendorf A (2015) Physiological mechanisms of adaptation of *Dianthus carthusianorum* L. to growth on a Zn-Pb waste deposit - the case of chronic multi-metal and acute Zn stress. Plant Soil 390: 237-250

Xu S, Li J, Zhang X, Wei H, Cui L (2006) Effects of heat acclimation pretreatment on changes of membrane lipid peroxidation, antioxidant metabolites, and ultrastructure of chloroplasts in two cool-season turfgrass species under heat stress. Environ Exp Bot 56: 274-285

Yu H, Huang Z, Ge C, Jiao P, Chen M, Li C (2013) Effect of lead and cadmium combined stress on growth and response of *Panicum maximum* in tropical soil. Fresenius Environ Bull 22: 808-812

Zare AA, Khoshgoftarmanesh AH, Malakouti MJ, Bahrami HA, Chaney RL (2018) Root uptake and shoot accumulation of cadmium by lettuce at various Cd:Zn ratios in nutrient solution. Ecotox Environ Safe 148: 441-446

Supporting information

Additional supporting information may be found online in the Supporting Information section at the end of the article.

Fig. S1. Leaf blade thickness and diameter of the root vascular center.

Fig. S2. $\delta^{15}N$ in the leaf blades, stems and sheaths and roots.

Fig. S3. Nutrient use efficiency.

Fig. S4. Total soluble protein concentration in the leaf blades.

Table S1. Nutrients content in the leaf blades, stems and sheaths and roots.

Figure legends

Fig. 1. Fresh biomass production (A-C), dry biomass production (D-F) and water content (G-I) in the leaf blades (top row), stems and sheaths (middle row) and roots (bottom row) of *Brachiaria decumbens* Stapf. cv. Basilisk and *Panicum maximum* Jacq. cv. Massai grown in the Cd-unpolluted (0.63 mg kg^{-1}) and Cd-polluted (3.60 mg kg^{-1}) Oxisol, in summer and winter conditions. Distinct uppercase letters indicate difference between seasons within each Cd concentration for each plant species, and distinct lowercase letters indicate difference between Cd concentrations within each season for each plant species (Tukey test, $P \leq 0.05$, n=4).

Fig. 2. Cadmium concentrations (A-C) and Cd contents (D-F) in the leaf blades (top row), stems and sheaths (middle row) and roots (bottom row) of *Brachiaria decumbens* Stapf. cv. Basilisk and *Panicum maximum* Jacq. cv. Massai grown in the Cd-unpolluted (0.63 mg kg^{-1}) and Cd-polluted (3.60 mg kg^{-1}) Oxisol, in summer and winter conditions. Distinct uppercase letters indicate difference between seasons within each Cd concentration for each plant species, and distinct lowercase letters indicate difference between Cd concentrations within each season for each plant species (Tukey test, $P \leq 0.05$, n=4).

Fig. 3. Cadmium concentrations in the root apoplast (A) and root symplast (B) and Cd partitioning between root apoplast and symplast (C) of *Brachiaria decumbens* Stapf. cv. Basilisk and *Panicum maximum* Jacq. cv. Massai grown in the Cd-unpolluted (0.63 mg Cd kg^{-1}) and Cd-polluted (3.60 mg Cd kg^{-1}) Oxisol, in summer and winter conditions. Distinct uppercase letters indicate difference between seasons within each Cd concentration for each plant species, and distinct lowercase letters indicate difference between Cd concentrations within each season for each plant species (Tukey test, $P \leq 0.05$, n=4).

Fig. 4. Morpho-anatomical changes and elemental composition (hair root zone) in the roots of *Brachiaria decumbens* Stapf. cv. Basilisk (A-H) and *Panicum maximum* Jacq. cv. Massai (I-P) grown in the Cd-unpolluted (0.63 mg kg^{-1}, A, C, E, G, I, K, M and O) and Cd-polluted (3.60 mg kg^{-1}; B, D, F, H, J, L, N and P) Oxisol in summer and winter conditions (summer = A, B, E, F, I, J, M and N and winter = C, D, G, H, K, L, O and P). Scanning electron microscopy (A-P): co, cortex; vc, vascular center; en, endodermis; mx, metaxylem; mp, medular parenchyma; pe, pericycle; rh, root hair; arrows show disorganization of cambial region. Bars: A-D, I-L = 100 µm; E-H, M-P = 50 µm.

Fig. 5. Cysteine (A-C), γ-glutamylcysteine (γ-EC, D-F), reduced glutathione (GSH, G-I) and total phytochelatins (PCs, J-L) concentrations in the leaf blades (top row), stems and sheaths (middle row) and roots (bottom row) of *Brachiaria decumbens* Stapf. cv. Basilisk and *Panicum maximum* Jacq. cv. Massai grown in the Cd-unpolluted (Unp., 0.63 mg kg^{-1}) and Cd-polluted (Cd, 3.60 mg kg^{-1}) Oxisol, in summer and winter conditions. Distinct uppercase letters indicate difference between seasons within each Cd concentration for each plant species, and distinct lowercase letters indicate difference between

Cd concentrations within each season for each plant species (Tukey test, $P \leq 0.05$, n=4). ND, non-detected.

Fig. 6. Concentrations of hydrogen peroxide (H_2O_2, A-C) and malondialdehyde (MDA, D-F) in the leaf blades (top row), stems and sheaths (middle row) and roots (bottom row) of *Brachiaria decumbens* Stapf. cv. Basilisk and *Panicum maximum* Jacq. cv. Massai grown in the Cd-unpolluted (0.63 mg kg^{-1}) and Cd-polluted (3.60 mg kg^{-1}) Oxisol, in summer and winter conditions. Distinct uppercase letters indicate difference between seasons within each Cd concentration for each plant species, and distinct lowercase letters indicate difference between Cd concentrations within each season for each plant species (Tukey test, $P \leq 0.05$, n=4).

Fig. 7. Total activities of the enzymes superoxide dismutase (SOD, A), catalase (CAT, B), ascorbate peroxidase (APX, C), guaiacol peroxidase (GPX, D) and glutathione reductase (GR, E) in the leaf blades of *Brachiaria decumbens* Stapf. cv. Basilisk and *Panicum maximum* Jacq. cv. Massai grown in the Cd-unpolluted (0.63 mg kg^{-1}) and Cd-polluted (3.60 mg kg^{-1}) Oxisol, in summer and winter conditions. Distinct uppercase letters indicate difference between seasons within each Cd concentration for each plant species, and distinct lowercase letters indicate difference between Cd concentrations within each season for each plant species (Tukey test, $P \leq 0.05$, n=4).

Fig. 8. Anatomical and ultrastructural changes in the leaf blades of *Brachiaria decumbens* Stapf. cv. Basilisk (A-L) and *Panicum maximum* Jacq. cv. Massai (M-X) grown in the Cd-unpolluted (0.63 mg kg^{-1}) = A, C, E, G, M, O, Q and S; and Cd-polluted (3.60 mg kg^{-1}) Oxisol = B, D, F, H-L, N, P, R and T-X; in summer and winter conditions (summer - A, B, E, F, I, J, M, N, Q, R, U and V; and winter - C, D, G, H, K, L, O, P, S, T, W and X). **Light microscopy (A-D and M-P):** bc: buliform cell; ch: chloroplast; ep: epidermis; vs: vascular system; is: intracellular space; arrows indicate starch grains. **Transmission electron microscopy (E-L and Q-X):** ch: chloroplast; mi: mitochondria; sg: starch grain; th: thylakoids; va: vacuole; smaller arrows show the presence of plastoglobules and larger arrows show disorders in the chloroplasts membrane containing small vesicles in *B. decumbens* Stapf. cv. Basilisk; smaller arrows show membrane rupture and larger arrows show peroxisomes, distorted thylakoids and presence of vesicles in *P. maximum* Jacq. cv. Massai, while asterisks (*) show the presence of electrodense material. Bars: A-D, M-P = 50 µm; E, I, G, K, Q, U, S, W = 1 µm; F, J, H, L, R, V, T, X = 0.5 µm.

Fig. 9. Leaf area (A), leaf CO_2 assimilation - A (B), stomatal conductance - g_s (C), intracellular CO_2 concentration - C_i (D), transpiration - E (E), instantaneous carboxylation efficiency - k (F), instantaneous water use efficiency - WUE (G), intrinsic water use efficiency - WUE_i (H), chlorophyll *a* concentration (I), chlorophyll *b* concentration (J), chlorophyll *a* + *b* concentration (K) and chlorophyll *a*/*b* ratio (L) of *Brachiaria decumbens* Stapf. cv. Basilisk and *Panicum maximum* Jacq. cv.

Massai grown in the Cd-unpolluted (0.63 mg kg^{-1}) and Cd-polluted (3.60 mg kg^{-1}) Oxisol, in summer and winter conditions. Distinct uppercase letters indicate difference between seasons within each Cd concentration for each plant species, and distinct lowercase letters indicate difference between Cd concentrations within each season for each plant species (Tukey test, $P \leq 0.05$, n=4). FIC - Falker chlorophyll index.

Table 1. Nutrients concentration in the leaf blades, stems and sheaths, and roots of *Brachiaria decumbens* Stapf. cv. Basilisk and *Panicum maximum* Jacq. cv. Massai grown in the Cd-unpolluted (0.63 mg kg^{-1}) and Cd-polluted (3.60 mg kg^{-1}) Oxisol, in summer and winter conditions.

Plant species	*B. decumbens*				*P. maximum*			
Season	Summer		Winter		Summer		Winter	
Oxisol	Cd-unpolluted	Cd-polluted	Cd-unpolluted	Cd-polluted	Cd-unpolluted	Cd-polluted	Cd-unpolluted	Cd-polluted
Leaf blades								
N (g kg^{-1} DW)	33.25 ± 1.62 Aa	34.37 ± 2.76 Aa	35.80 ± 1.88 Aa	36.47 ± 1.73 Aa	20.65 ± 0.51 Aa	22.70 ± 0.55 Aa	24.25 ± 0.54 Aa	25.27 ± 0.74 Aa
P (g kg^{-1} DW)	3.82 ± 0.18 Aa	3.88 ± 0.38 Aa	3.29 ± 0.21 Ab	4.26 ± 0.06 Aa	2.91 ± 0.22 Aa	2.34 ± 0.45 Aa	2.46 ± 0.10 Aa	2.56 ± 0.10 Aa
K (g kg^{-1} DW)	34.58 ± 0.83 Aa	34.08 ± 2.77 Aa	25.53 ± 1.08 Bb	30.07 ± 0.62 Ba	16.55 ± 0.46 Aa	19.65 ± 0.67 Aa	18.69 ± 0.55 Aa	21.89 ± 0.35 Aa
Ca (g kg^{-1} DW)	7.51 ± 0.68 Aa	6.20 ± 0.39 Ba	7.37 ± 0.69 Aa	8.92 ± 0.47 Aa	7.33 ± 0.92 Aa	7.39 ± 0.35 Aa	6.80 ± 0.35 Aa	5.83 ± 0.44 Aa
Mg (g kg^{-1} DW)	5.58 ± 0.13 Aa	5.02 ± 0.39 Aa	4.87 ± 0.39 Aa	5.08 ± 0.41 Aa	3.34 ± 0.09 Aa	3.29 ± 0.15 Aa	3.23 ± 0.11 Aa	3.15 ± 0.24 Aa
S (g kg^{-1} DW)	2.86 ± 0.06 Aa	2.84 ± 0.23 Aa	2.51 ± 0.10 Aa	2.84 ± 0.16 Aa	1.72 ± 0.13 Aa	1.86 ± 0.06 Aa	1.86 ± 0.05 Aa	1.72 ± 0.07 Aa
B (mg kg^{-1} DW)	25.60 ± 4.02 Aa	20.23 ± 2.73 Aa	24.37 ± 3.64 Aa	17.80 ± 2.62 Aa	21.27 ± 2.07 Aa	10.44 ± 2.18 Ab	11.05 ± 0.27 Ba	10.72 ± 0.96 Aa
Cu (mg kg^{-1} DW)	6.32 ± 0.50 Aa	5.52 ± 0.44 Aa	5.05 ± 0.42 Ba	4.85 ± 0.26 Aa	3.75 ± 0.10 Aa	4.15 ± 0.26 Aa	3.83 ± 0.13 Aa	3.05 ± 0.27 Ba
Fe (mg kg^{-1} DW)	314.80 ± 47.34 Aa	352.49 ± 20.26 Aa	309.71 ± 29.21 Ab	425.97 ± 43.82 Aa	257.63 ± 19.35 Aa	242.81 ± 5.71 Aa	245.46 ± 7.98 Aa	164.77 ± 14.17 Aa
Mn (mg kg^{-1} DW)	730.99 ± 13.56 Aa	669.49 ± 58.76 Aa	678.21 ± 39.23 Aa	719.32 ± 52.18 Aa	456.30 ± 7.59 Aa	499.45 ± 50.86 Aa	512.87 ± 28.55 Aa	540.78 ± 21.73 Aa
Mo (mg kg^{-1} DW)	0.094 ± 0.028 Aa	0.072 ± 0.008 Aa	0.066 ± 0.010 Aa	0.058 ± 0.004 Aa	0.097 ± 0.027 Aa	0.112 ± 0.024 Aa	0.042 ± 0.010 Ba	0.058 ± 0.010 Aa
Zn (mg kg^{-1} DW)	621.33 ± 45.54 Aa	436.19 ± 37.94 Ab	440.27 ± 47.67 Ba	480.53 ± 25.70 Aa	196.80 ± 23.70 Aa	227.36 ± 37.65 Aa	276.09 ± 17.91 Aa	187.94 ± 9.58 Aa
Stems and sheaths								
N (g kg^{-1} DW)	22.22 ± 0.80 Ba	22.32 ± 1.66 Ba	25.62 ± 0.98 Aa	27.00 ± 1.93 Aa	17.02 ± 0.22 Aa	17.47 ± 0.86 Aa	19.15 ± 0.18 Aa	19.70 ± 0.86 Aa
P (g kg^{-1} DW)	3.02 ± 0.17 Aa	3.18 ± 0.26 Ba	3.00 ± 0.22 Ab	3.94 ± 0.29 Aa	2.51 ± 0.07 Aa	2.44 ± 0.15 Aa	2.33 ± 0.12 Aa	2.62 ± 0.08 Aa
K (g kg^{-1} DW)	36.54 ± 2.12 Aa	35.37 ± 4.01 Aa	33.44 ± 2.38 Aa	34.57 ± 2.13 Aa	16.61 ± 1.03 Aa	18.13 ± 0.96 Ba	20.16 ± 0.73 Aa	25.04 ± 1.13 Aa
Ca (g kg^{-1} DW)	2.90 ± 0.33 Aa	2.70 ± 0.24 Aa	3.03 ± 0.12 Aa	3.24 ± 0.23 Aa	3.71 ± 0.17 Aa	3.89 ± 0.15 Aa	3.64 ± 0.18 Aa	3.47 ± 0.22 Aa
Mg (g kg^{-1} DW)	2.84 ± 0.13 Aa	2.92 ± 0.15 Aa	2.84 ± 0.21 Aa	3.00 ± 0.13 Aa	3.02 ± 0.11 Aa	2.73 ± 0.10 Ba	3.14 ± 0.20 Aa	3.41 ± 0.21 Aa
S (g kg^{-1} DW)	2.17 ± 0.12 Aa	2.17 ± 0.20 Aa	1.93 ± 0.17 Ab	2.42 ± 0.21 Aa	2.08 ± 0.15 Aa	2.21 ± 0.15 Aa	2.07 ± 0.13 Aa	2.00 ± 0.07 Aa
B (mg kg^{-1} DW)	11.41 ± 1.30 Aa	9.46 ± 0.38 Aa	13.13 ± 1.39 Aa	9.88 ± 1.07 Aa	20.86 ± 3.47 Aa	10.78 ± 0.99 Ab	11.81 ± 2.04 Ba	8.03 ± 0.95 Aa
Cu (mg kg^{-1} DW)	3.79 ± 0.38 Aa	3.68 ± 0.31 Aa	3.88 ± 0.26 Aa	4.32 ± 0.30 Aa	2.73 ± 0.10 Aa	2.92 ± 0.18 Aa	2.66 ± 0.13 Aa	2.91 ± 0.15 Aa
Fe (mg kg^{-1} DW)	418.47 ± 84.84 Aa	528.94 ± 27.73 Aa	508.24 ± 51.22 Ab	733.82 ± 117.44 Aa	611.30 ± 62.93 Bb	840.09 ± 80.04 Aa	861.40 ± 127.73 Aa	665.65 ± 53.49 Aa
Mn (mg kg^{-1} DW)	353.54 ± 4.37 Aa	382.75 ± 13.37 Aa	391.39 ± 25.55 Aa	376.18 ± 12.52 Aa	589.25 ± 31.55 Aa	619.55 ± 55.54 Aa	591.80 ± 45.68 Aa	680.12 ± 15.87 Aa
Mo (mg kg^{-1} DW)	0.057 ± 0.011 Aa	0.092 ± 0.010 Aa	0.097 ± 0.022 Aa	0.080 ± 0.014 Aa	0.160 ± 0.025 Aa	0.205 ± 0.023 Aa	0.087 ± 0.023 Ba	0.142 ± 0.021 Ba
Zn (mg kg^{-1} DW)	970.96 ± 52.19 Aa	1048.87 ± 64.80 Aa	881.09 ± 16.53 Ab	1142.29 ± 60.29 Aa	1136.21 ± 17.31 Aa	1155.20 ± 129.81 Aa	1086.06 ± 87.79 Aa	1263.21 ± 104.50 Aa
Roots								
N (g kg^{-1} DW)	13.60 ± 1.46 Aa	11.65 ± 1.97 Ba	16.05 ± 0.65 Ab	19.85 ± 2.96 Aa	7.72 ± 0.42 Aa	7.50 ± 0.45 Aa	10.87 ± 0.37 Aa	11.12 ± 1.10 Aa
P (g kg^{-1} DW)	1.38 ± 0.15 Aa	1.05 ± 0.17 Bb	1.14 ± 0.05 Ab	1.65 ± 0.21 Aa	0.88 ± 0.03 Aa	0.98 ± 0.06 Aa	1.07 ± 0.06 Aa	0.95 ± 0.07 Aa
K (g kg^{-1} DW)	10.16 ± 0.86 Ba	6.51 ± 0.73 Bb	14.79 ± 0.61 Aa	14.79 ± 0.39 Aa	5.47 ± 0.24 Ba	5.58 ± 0.11 Ba	9.89 ± 1.07 Aa	11.83 ± 1.30 Aa
Ca (g kg^{-1} DW)	2.39 ± 0.41 Aa	1.76 ± 0.15 Bb	2.55 ± 0.18 Aa	2.97 ± 0.19 Aa	1.47 ± 0.11 Aa	1.42 ± 0.13 Aa	1.89 ± 0.20 Aa	1.55 ± 0.03 Aa
Mg (g kg^{-1} DW)	2.68 ± 0.30 Aa	1.98 ± 0.36 Ba	2.49 ± 0.30 Aa	3.20 ± 0.29 Aa	0.61 ± 0.05 Aa	0.68 ± 0.07 Aa	1.02 ± 0.20 Aa	1.20 ± 0.18 Aa
S (g kg^{-1} DW)	1.63 ± 0.08 Aa	1.20 ± 0.25 Bb	1.31 ± 0.13 Ab	1.82 ± 0.28 Aa	0.62 ± 0.02 Aa	0.89 ± 0.05 Aa	0.84 ± 0.06 Aa	0.89 ± 0.05 Aa
B (mg kg^{-1} DW)	44.64 ± 8.37 Aa	42.83 ± 3.26 Aa	60.80 ± 9.39 Aa	21.42 ± 1.90 Bb	41.35 ± 6.89 Aa	21.82 ± 1.76 Ab	29.93 ± 3.27 Aa	17.10 ± 2.95 Aa
Cu (mg kg^{-1} DW)	7.65 ± 0.33 Aa	6.73 ± 0.56 Aa	5.91 ± 0.48 Ab	8.19 ± 0.77 Aa	3.72 ± 0.56 Ba	4.83 ± 0.38 Aa	5.72 ± 0.46 Aa	4.59 ± 0.24 Aa
Fe (mg kg^{-1} DW)	5418.13 ± 384.42 Aa	5629.13 ± 371.73 Aa	3345.36 ± 447.40 Bb	4566.13 ± 434.88 Ba	2606.22 ± 324.60 Aa	3105.73 ± 336.48 Aa	3747.69 ± 394.95 Aa	2854.68 ± 299.03 Aa
Mn (mg kg^{-1} DW)	296.06 ± 35.20 Aa	233.53 ± 21.01 Ab	246.96 ± 7.44 Ba	257.29 ± 13.18 Aa	112.40 ± 10.55 Aa	138.47 ± 10.05 Aa	166.42 ± 7.41 Aa	147.99 ± 4.91 Aa
Mo (mg kg^{-1} DW)	0.32 ± 0.013 Aa	0.30 ± 0.013 Aa	0.24 ± 0.031 Aa	0.30 ± 0.027 Aa	0.19 ± 0.039 Ba	0.22 ± 0.048 Aa	0.33 ± 0.036 Aa	0.27 ± 0.039 Aa
Zn (mg kg^{-1} DW)	1563.79 ± 94.41 Aa	1040.58 ± 84.79 Bb	1062.00 ± 45.44 Bb	1324.62 ± 8.44 Aa	308.04 ± 43.86 Ba	325.34 ± 38.11 Aa	582.78 ± 68.15 Aa	480.53 ± 17.44 Aa

Means ± SEM followed by distinct uppercase letters in rows indicate difference between seasons within each Cd concentration for each plant species, and distinct lowercase letters in rows indicate difference between Cd concentrations within each season for each plant species (Tukey test, $p \leq 0.05$).

Leaf blades →

Stems and sheaths →

Roots →

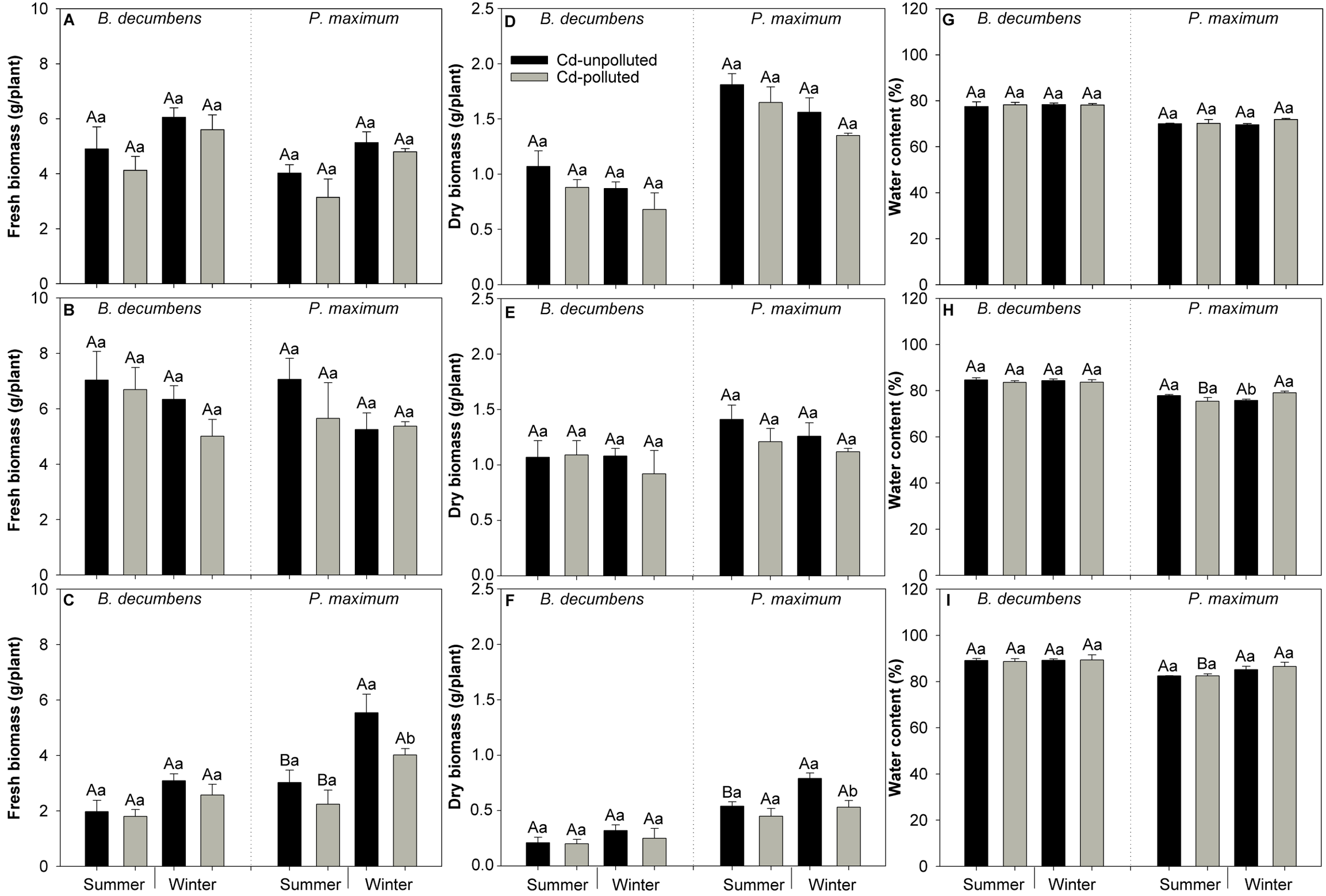

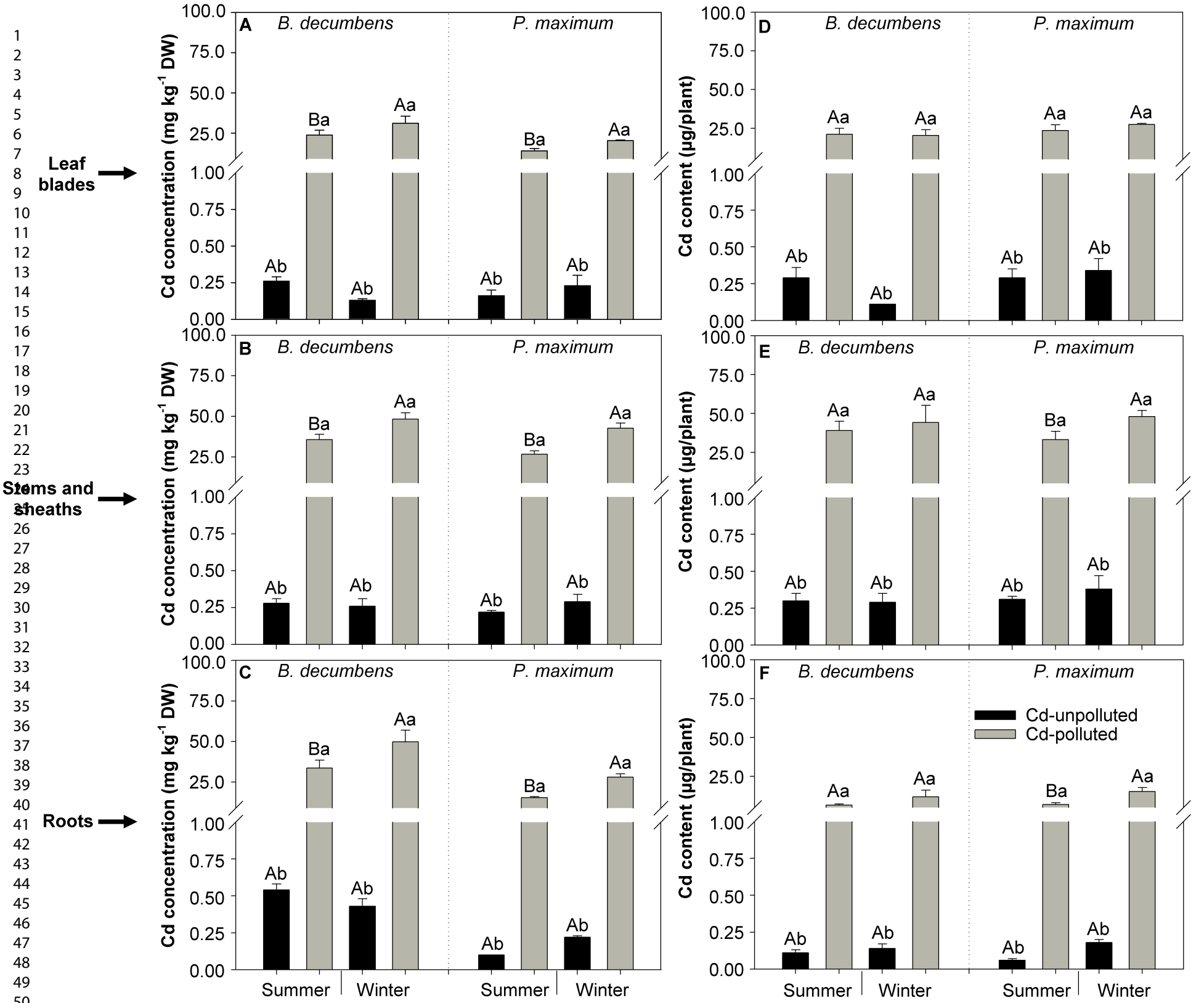
A
B
C
D
E
F
B. decumbens
P. maximum
Cd concentration (mg kg-1 DW)
Cd content (µg/plant)
Leaf blades
Stems and sheaths
Roots
Cd-unpolluted
Cd-polluted
Summer
Winter
Ab
Ba
Aa

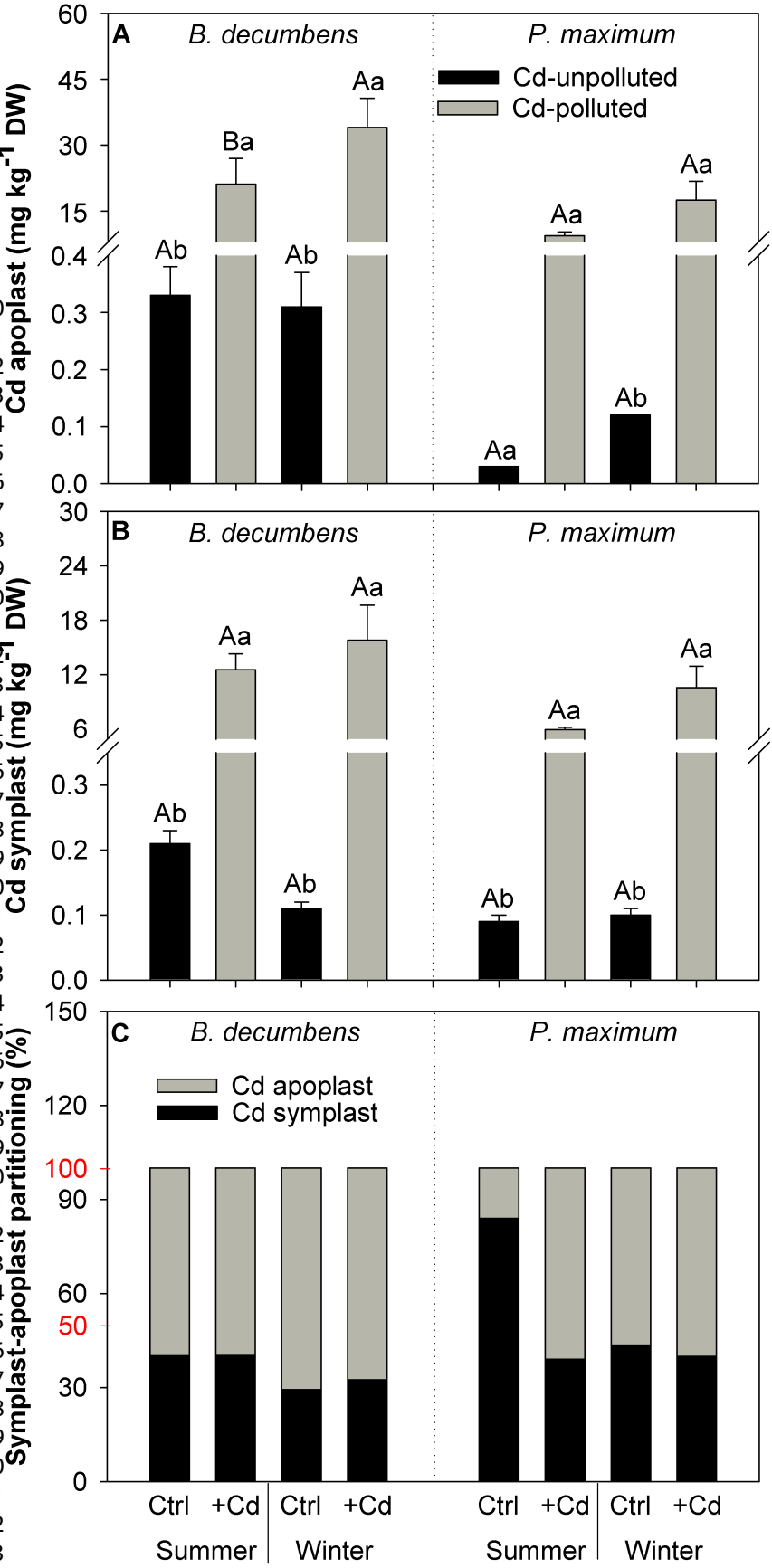
A
B. decumbens
P. maximum
Cd-unpolluted
Cd-polluted
Cd apoplast (mg kg-1 DW)
60
45
30
15
0.4
0.3
0.2
0.1
0.0
Ab
Ba
Aa
Ab
Aa
Aa
Ab
Aa
B
B. decumbens
P. maximum
Cd symplast (mg kg-1 DW)
30
24
18
12
6
0.3
0.2
0.1
0.0
Ab
Aa
Ab
Aa
Ab
Aa
Ab
C
B. decumbens
P. maximum
Cd apoplast
Cd symplast
Symplast-apoplast partitioning (%)
150
120
100
90
60
50
30
0
Ctrl
+Cd
Ctrl
+Cd
Ctrl
+Cd
Ctrl
+Cd
Summer
Winter
Summer
Winter

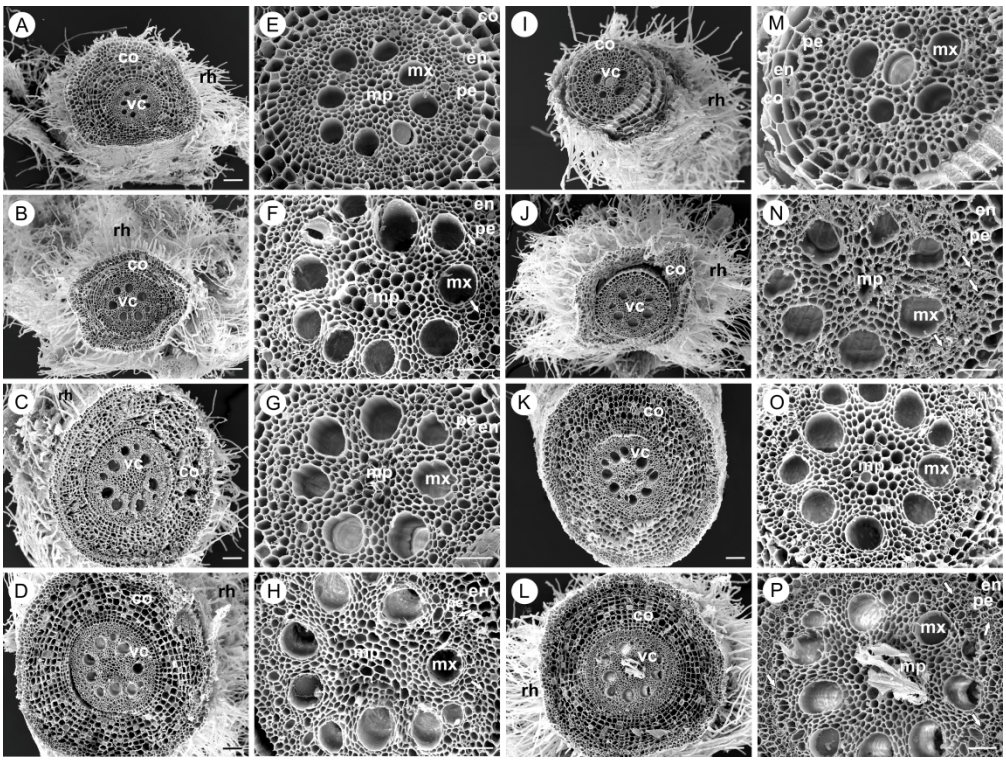
A
co
rh
vc
E
co
mx
en
mp
pe
I
co
vc
rh
M
pe
mx
en
co
B
rh
co
vc
F
en
pe
mx
mp
J
co
rh
vc
N
en
pe
mp
mx
C
rh
vc
co
G
pe
en
mp
mx
K
co
vc
O
mp
mx
D
co
rh
vc
H
en
mp
mx
L
co
vc
rh
P
en
pe
mx
mp

Figure 4

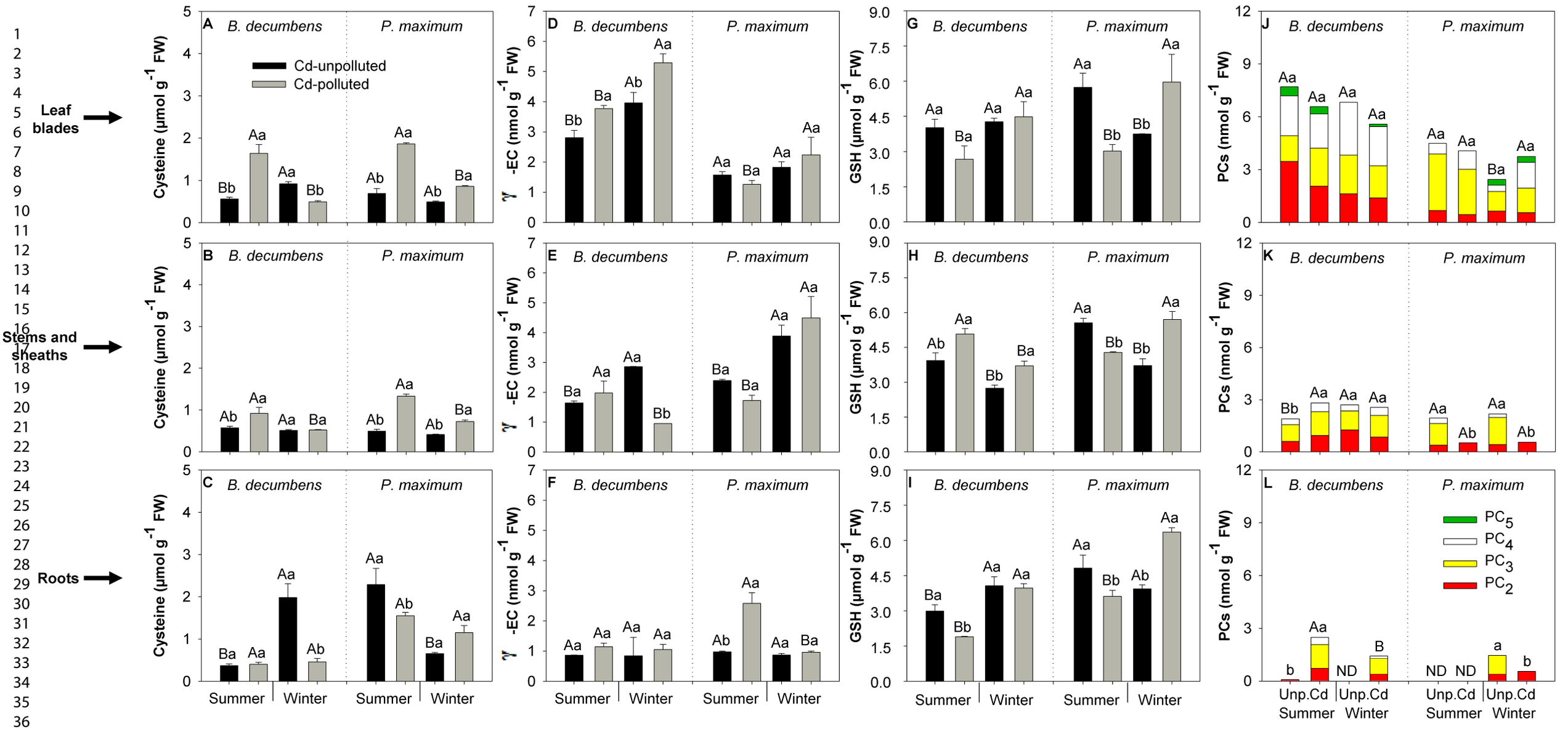
Leaf blades
Stems and sheaths
Roots
A B. decumbens P. maximum
Cd-unpolluted
Cd-polluted
Cysteine (µmol g-1 FW)
γ -EC (nmol g-1 FW)
GSH (µmol g-1 FW)
PCs (nmol g-1 FW)
Summer
Winter
Unp.Cd
PC5
PC4
PC3
PC2
ND

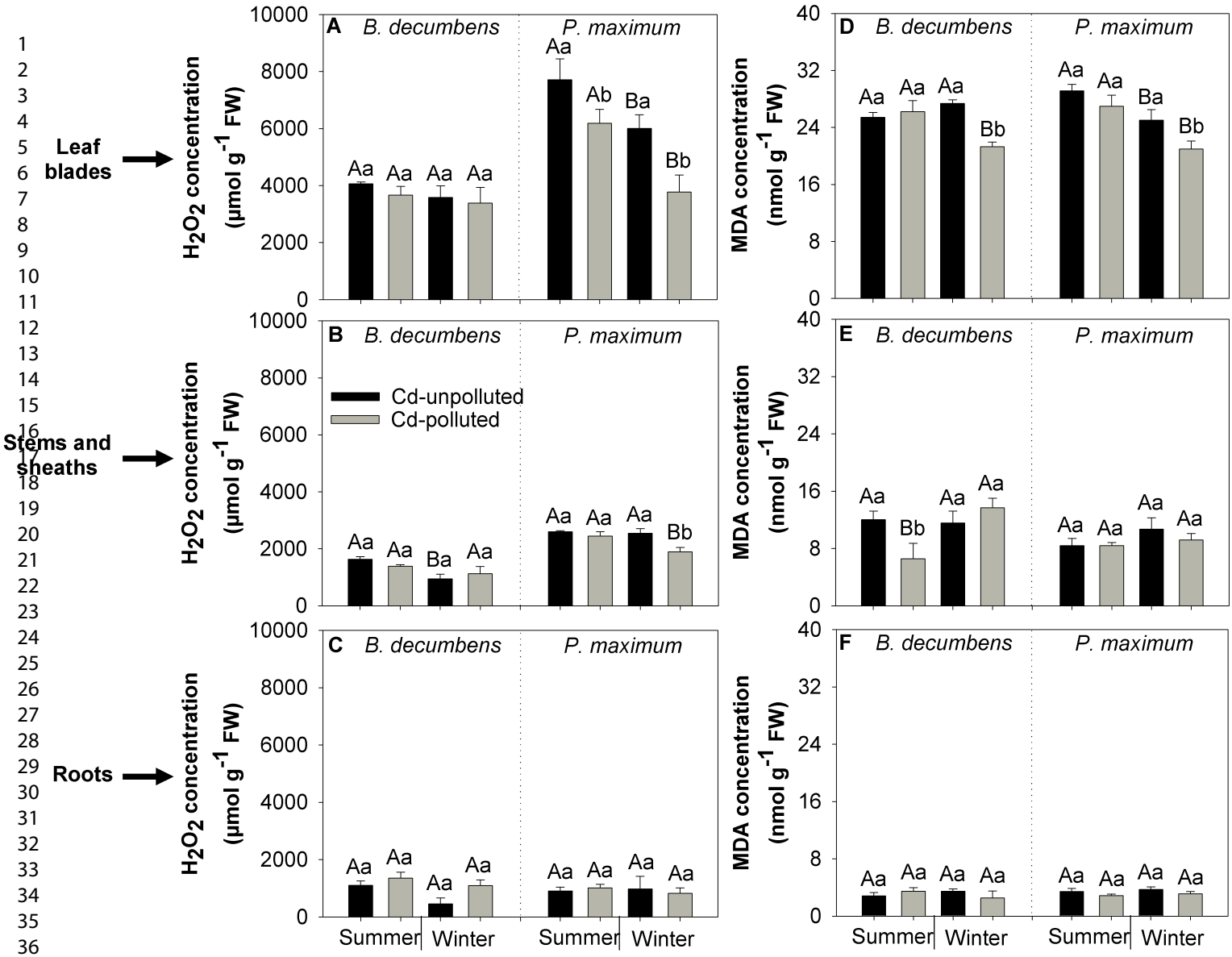
Leaf blades
Stems and sheaths
Roots
A
B
C
D
E
F
B. decumbens
P. maximum
Cd-unpolluted
Cd-polluted
H2O2 concentration (µmol g-1 FW)
MDA concentration (nmol g-1 FW)
Summer
Winter

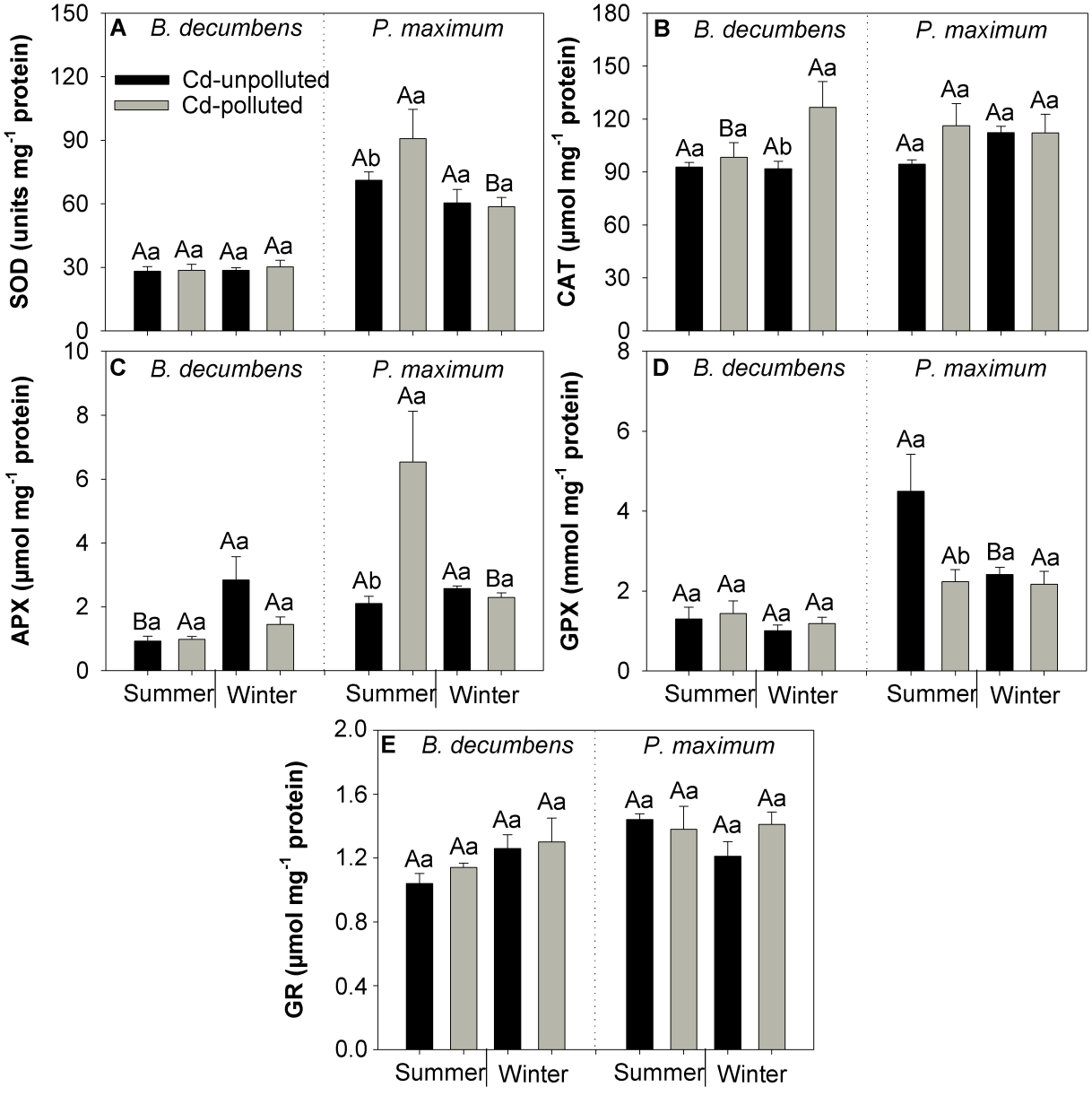
A
B. decumbens
P. maximum
Cd-unpolluted
Cd-polluted
SOD (units mg-1 protein)
B
CAT (µmol mg-1 protein)
C
APX (µmol mg-1 protein)
D
GPX (mmol mg-1 protein)
E
GR (µmol mg-1 protein)
Summer
Winter

Brachiaria decumbens

Panicum maximum

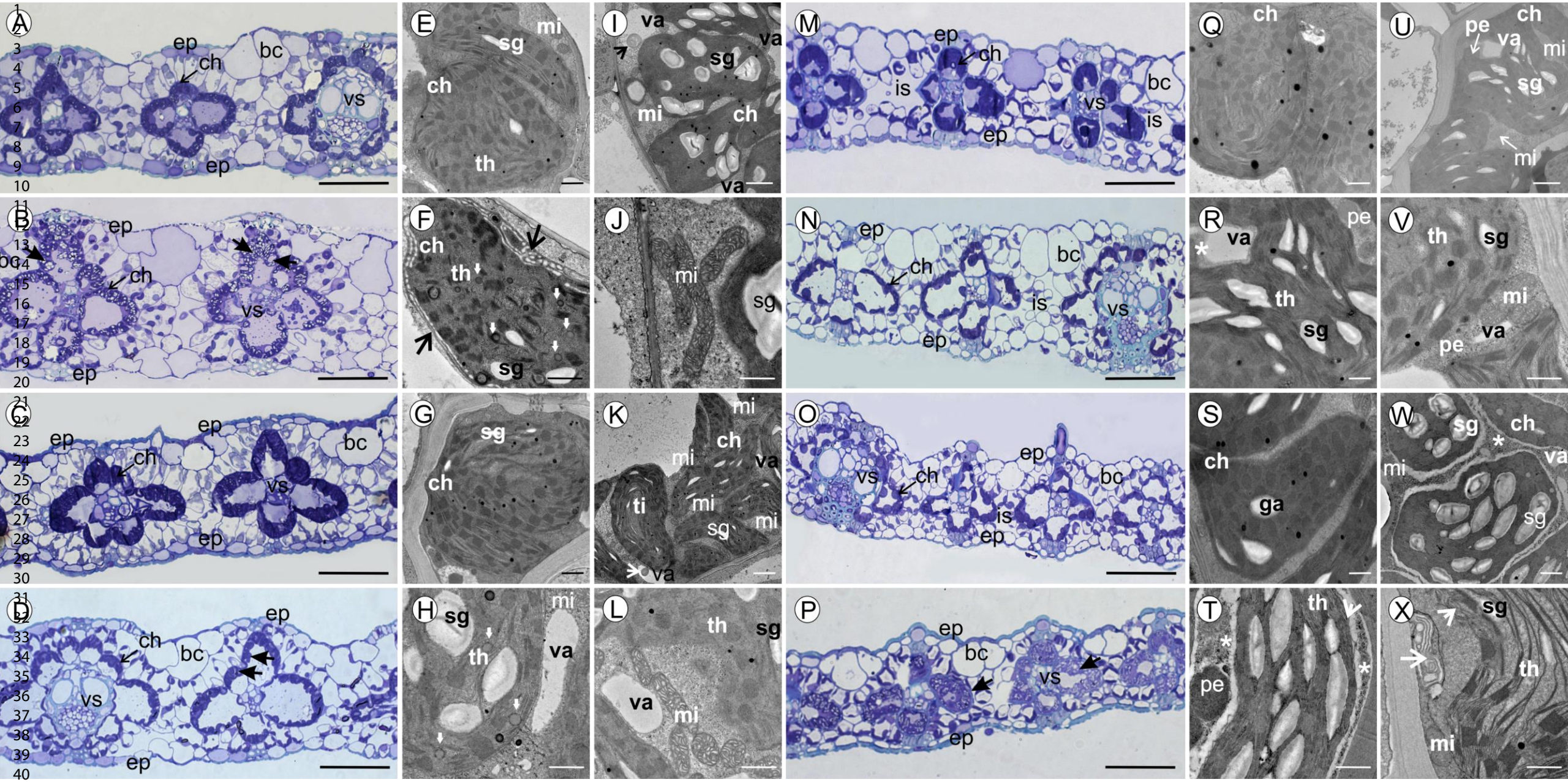

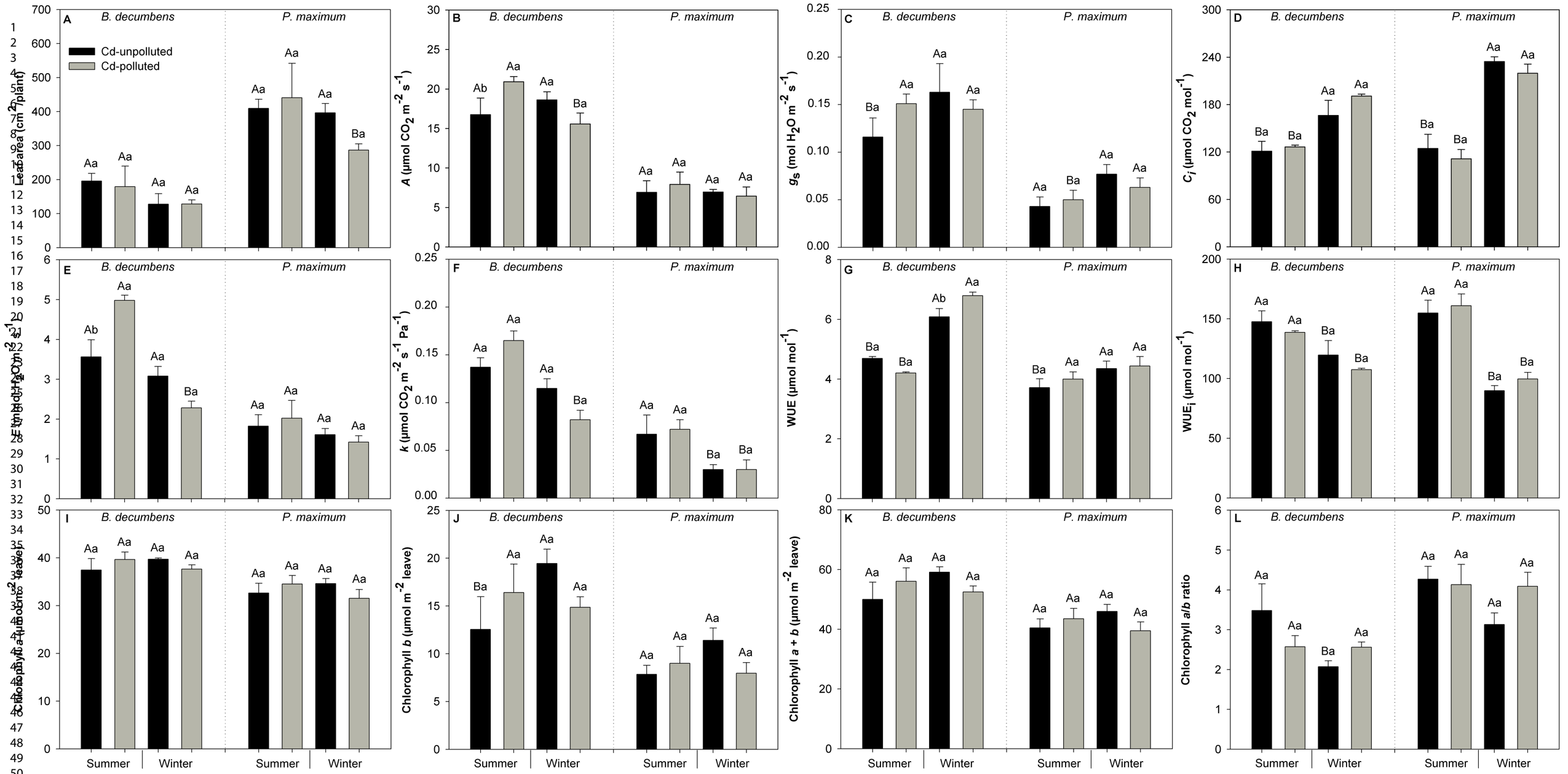
A
B. decumbens
P. maximum
Cd-unpolluted
Cd-polluted
Leaf area (cm²/plant)
B
A (μmol CO2 m-2 s-1)
C
gs (mol H2O m-2 s-1)
D
Ci (μmol CO2 mol-1)
E
Transpiration rate (mmol H2O m-2 s-1)
F
k (μmol CO2 m-2 s-1 Pa-1)
G
WUE (μmol mol-1)
H
WUEi (μmol mol-1)
I
Chlorophyll a (μmol m-2 leave)
J
Chlorophyll b (μmol m-2 leave)
K
Chlorophyll a + b (μmol m-2 leave)
L
Chlorophyll a/b ratio
Summer
Winter